TMEX-2020, Quy Nhon, Vietnam

Cosmic ray feedback in star-formation and implications for gamma-ray emission from starbursts

Roland Crocker

ANU

Australian National University

Describing these works:

- *'Cosmic ray transport in starburst galaxies';*
  Krumholz, Crocker, Xu, Lazarian, Robertson & Bedwell (2019), *in submission,* MNRAS (1911.09774)

- *'Cosmic Ray Feedback Bounds the Star Formation Efficiency of Spiral Galaxies';*
  Crocker, Krumholz, Thompson, et al. (2020); *in preparation*

Two Claims

A correct understanding of cosmic ray transport in (relatively) dense, partially ionised (but largely neutral) gas allows us to

1. Make sense of the observed gamma-ray spectra of some nearby starbursts and their empirically-demanded CR loss timescales

2. Make sense of the fact that there is an empirical upper limit to the star formation of 'normal' galaxies

Cosmic Rays

- Cosmic rays can be measured locally and their presence throughout the Galactic disk can be inferred from its gamma-ray emission

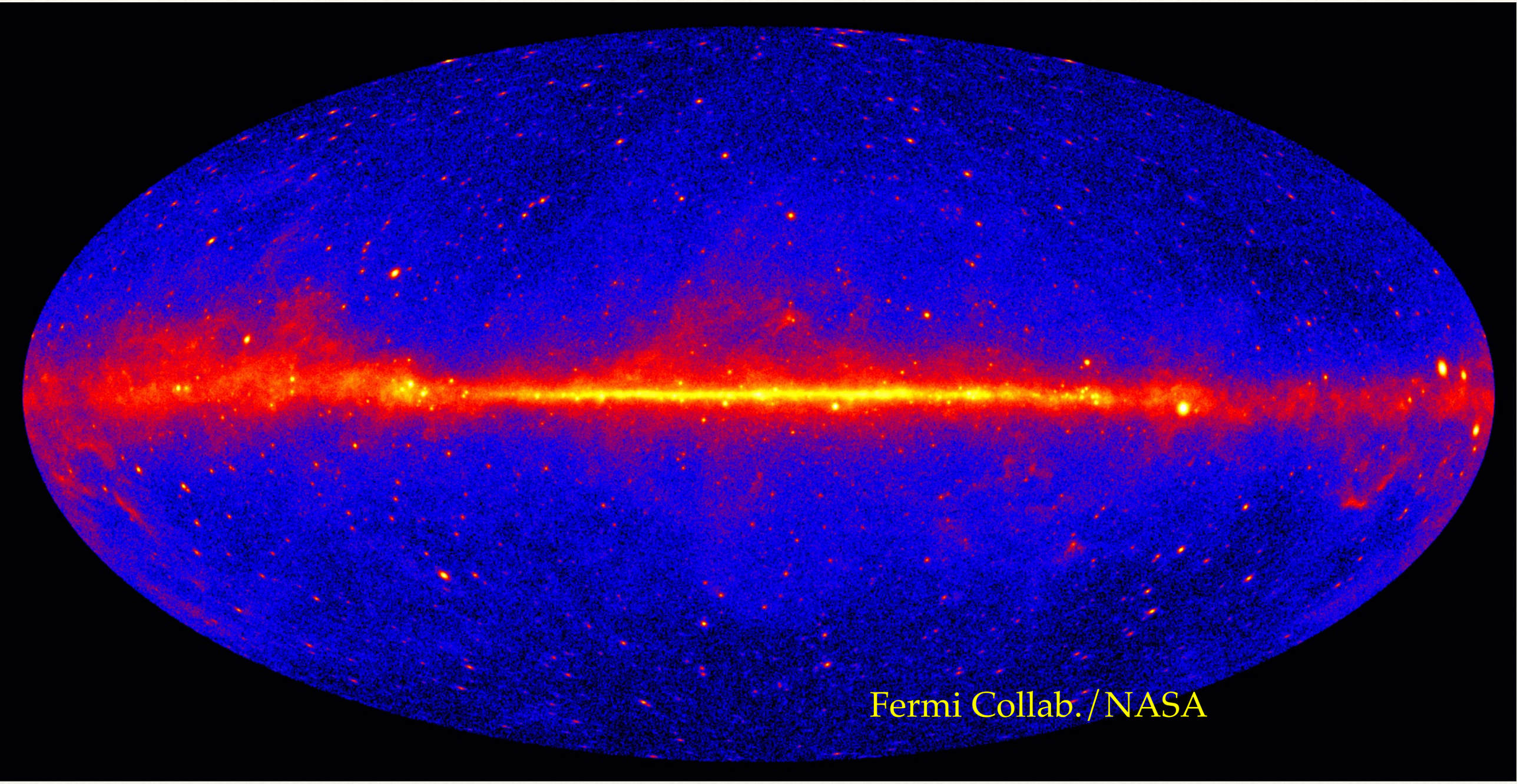
Fermi Collab./NASA

Cosmic Rays

- Cosmic rays can be measured locally and their presence throughout the Galactic disk can be inferred from its gamma-ray emission
- Similarly, we know from gamma-ray observations that there are diffuse cosmic ray populations suffusing the disks of external, star-forming galaxies (local group, nearby starbursts)

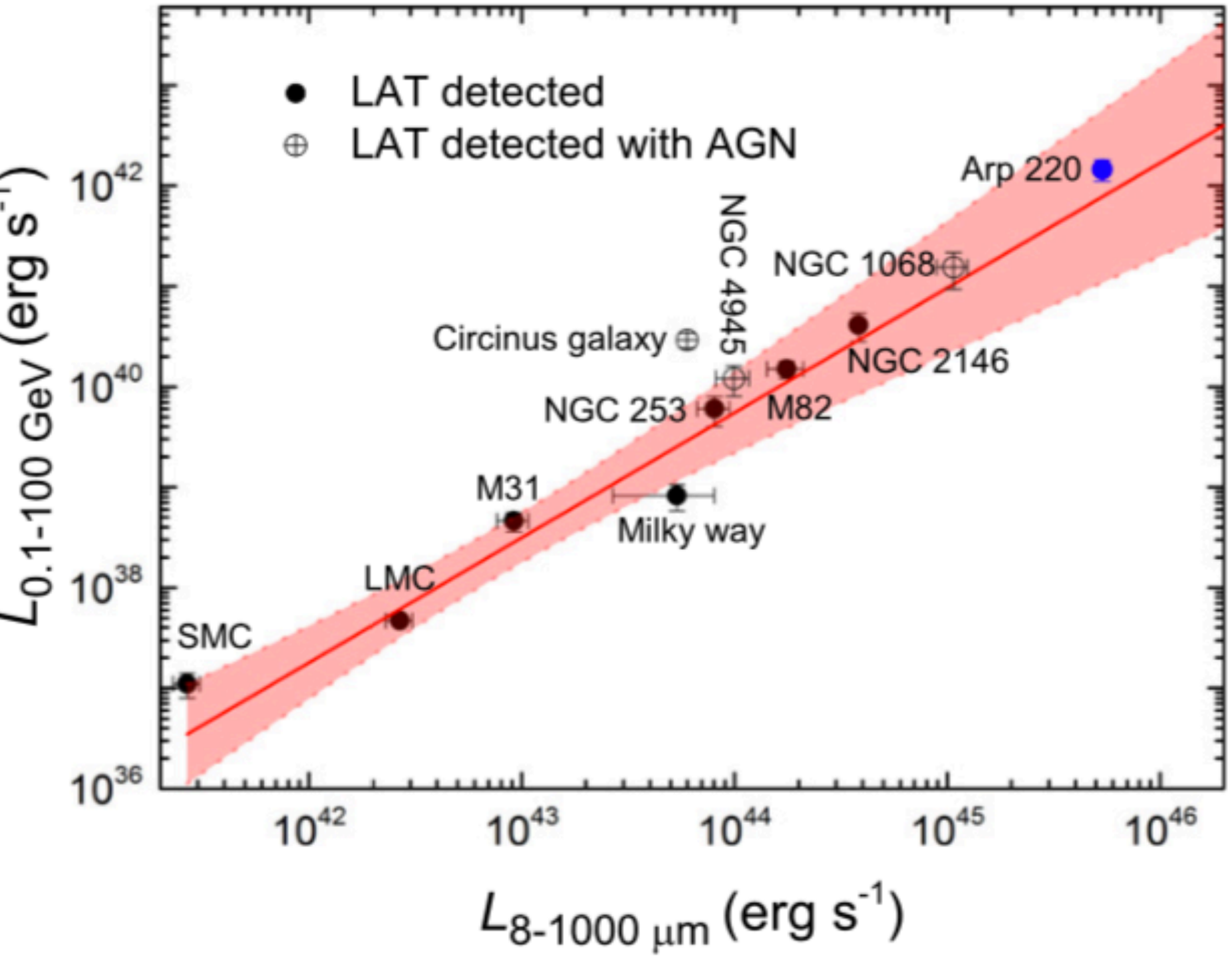

Peng+2016

total infrared luminosity data are taken from Gao & Solomon (2004), and γ-ray luminosities are taken from Ackermann et al. (2012) and Tang et al. (2014)

Cosmic Rays

- Cosmic rays can be measured locally and their presence throughout the Galactic disk can be inferred from its gamma-ray emission
- Similarly, we know from gamma-ray observations that there are diffuse cosmic ray populations suffusing the disks of external, star-forming galaxies (local group, nearby starbursts)
- As CRs scatter on B field they exchange momentum with the B field

Cosmic Rays

- Cosmic rays can be measured locally and their presence throughout the Galactic disk can be inferred from its gamma-ray emission
- Similarly, we know from gamma-ray observations that there are diffuse cosmic ray populations suffusing the disks of external, star-forming galaxies (local group, nearby starbursts)
- As CRs scatter on B field they exchange momentum with the B field
- ⇒ they exert an effective pressure to the gas into which the B field is “frozen in”

CRs are dynamically important in galaxies:

- (hadronic gamma-ray emission ⇒) CRs suffuse the dense gas
- CRs inferred to dominate heating and ionisation of H_2

  ⇒ maintain temp of H_2 and ensure it is coupled to magnetic fields

  ⇒ affect star formation
- in the Milky Way, CRs provide energy density / pressure equivalent to other ISM phases (Boulares & Cox 1990)

  ⇒ CRs help to support the scale height of the gaseous disk
- CRs help launch galactic outflows (Ipavich 1975, Breitchwerdt +)

Cosmic Rays in the Milky Way (classical picture)

- CR transport in Galaxy ~ random walk
- CRs effectively diffuse with scattering length: $\lambda_{CR} \sim$ **pc**
- $\lambda_{CR} \gg r_g$

$$r_g = \frac{\gamma m c v \sin\alpha}{eB} \approx \frac{E_{CR} \sin\alpha}{eB} \sim 10^{-6}\ E_{CR,0}\ B_0^{-1}\ \mathrm{pc},$$

- At a heuristic level, λ_{CR} can be derived from quasi-linear theory in a picture where there is a ~Kolmogorov turbulence cascade from the ~100 pc turbulence injection scale down to the gyroradius scale
- CRs spend most of their time in ionised ISM, with ~kpc scale height

Cosmic Rays in the Milky Way (classical picture)

- CR transport in Galaxy ~ random walk
- CRs effectively diffuse with scattering length: $\lambda_{CR} \sim$ **pc**
- $\lambda_{CR} \gg r_g$

$$r_g = \frac{\gamma m c v \sin\alpha}{eB} \approx \frac{E_{CR} \sin\alpha}{eB} \sim 10^{-6}\ E_{CR,0}\ B_0^{-1}\ \text{pc},$$

GeV

- At a heuristic level, λ_{CR} can be derived from quasi-linear theory in a picture where there is a ~Kolmogorov turbulence cascade from the ~100 pc turbulence injection scale down to the gyroradius scale
- CRs spend most of their time in ionised ISM, with ~kpc scale height

Cosmic Rays in the Milky Way (classical picture)

- CR transport in Galaxy ~ random walk
- CRs effectively diffuse with scattering length: $\lambda_{CR} \sim$ **pc**
- $\lambda_{CR} \gg r_g$

$$r_g = \frac{\gamma m c v \sin\alpha}{eB} \approx \frac{E_{CR} \sin\alpha}{eB} \sim 10^{-6}\ E_{CR,0}\ B_0^{-1}\ \mathrm{pc},$$

GeV μG

- At a heuristic level, λ_{CR} can be derived from quasi-linear theory in a picture where there is a ~Kolmogorov turbulence cascade from the ~100 pc turbulence injection scale down to the gyroradius scale
- CRs spend most of their time in ionised ISM, with ~kpc scale height

CR Transport in 'Neutral' Gas

- The mid-planes of starbursts are dominated by cold, neutral gas, neutral gas filling factor → 100%
- ⇒ The ISM processes determining CR transport in starbursts are different to those operating at large scales in galaxies like the Milky Way.
- However, even for the MW, close to midplane, filling factor of `neutral' gas approaches 50%

CR Transport in 'Neutral' Gas

- Low ionisation fractions in this medium ⇒ damping of turbulence by **ion-neutral drag**. *This fundamentally changes the nature of CR transport* (Kulsrud & Pearce 1969, Lazarian 2016, Xu & Lazarian 2016,2017,2018).
- In particular, GeV CRs can***not*** scatter off the strong, large-scale turbulence found in starbursts, because efficient ion-neutral damping prevents such turbulence from cascading down to their ~10^{-6} pc gyroradius scale

Why does ion-neutral damping kill the turbulence cascade?

- The neutral gas is, in reality ionised at some level,

  ionization fraction (by mass): $\chi \sim 10^{-5} - 10^{-2}$

- For given ISM parameters, 3 different frequencies that must be compared:
  - frequency of a particular MHD wave: ν
  - ion-neutral collision frequency: ν_{in}
  - neutral-ion collision frequency: ν_{ni}
  - $\nu_{ni} = \chi \, \nu_{in}$

3 regimes

- $\nu \ll \nu_{ni} < \nu_{in}$, ***coupled:*** many collisions will occur per oscillation, forcing the ions and neutrals to move together, thus act as a **single magnetised fluid** supporting the usual family of MHD waves.

3 regimes

- $\nu \ll \nu_{ni} < \nu_{in}$, ***coupled:*** many collisions will occur per oscillation, forcing the ions and neutrals to move together, acting as a single magnetised fluid supporting the usual family of MHD waves.
- $\nu_{ni} < \nu_{in} \ll \nu$, ***decoupled:*** essentially no ion-neutral collisions during each oscillation period $\Rightarrow$ the medium acts like **two completely separate fluids**. MHD waves propagate only in the ions; decoupled sound waves propagate in neutrals.

3 regimes

- $\nu \ll \nu_{ni} < \nu_{in}$, ***coupled:*** many collisions will occur per oscillation, forcing the ions and neutrals to move together, acting as a single magnetised fluid supporting the usual family of MHD waves.
- $\nu_{ni} < \nu_{in} \ll \nu$, ***decoupled:*** essentially no ion-neutral collisions during each oscillation period ⇒ the medium acts like two completely separate fluids. MHD waves propagate only in the ions; decoupled sound waves propagate in neutrals.
- $\nu_{ni} < \nu < \nu_{in}$, ***damping:***
  - ions attempt to oscillate in response to perturbations in the magnetic field, but still collide with the surrounding neutrals. Thus, the ion-neutral collisions prevent the ions from oscillating freely.
  - neutrals, decoupled from ions due to their infrequent collisions with ions, cannot move with the Alfven waves.
  - the ion-neutral collisions will convert organised Alfven wave motions in the weakly coupled ions and neutrals into microscopic random motions, dissipating them into heat.

Implication

- The turbulence cascade in the ions cuts off at a damping scale

$$L_{\mathrm{damp,A}} = \frac{\pi}{\sqrt{2}L}\left(\frac{u_{\mathrm{LA}}}{\gamma_{\mathrm{d}}\chi\rho}\right)^{3/2}\min\left(1,\mathcal{M}_{\mathrm{A}}^{1/2}\right)$$

$$\approx \frac{0.0011}{L_2^{1/2}}\left(\frac{u_{\mathrm{LA},1}}{n_{\mathrm{H},3}\chi_{-4}}\right)^{3/2}\min\left(1,\mathcal{M}_{\mathrm{A}}^{1/2}\right)\ \mathrm{pc}$$

- ..much bigger than the GeV gyroradius

$$r_{\mathrm{g}} = \frac{\gamma mcv\sin\alpha}{eB} \approx \frac{E_{\mathrm{CR}}\sin\alpha}{eB} \sim 10^{-6}\ E_{\mathrm{CR},0}\ B_0^{-1}\ \mathrm{pc},$$

Implication

- The turbulence cascade in the ions cuts off at a damping scale

$$L_{\mathrm{damp,A}} = \frac{\pi}{\sqrt{2}L}\left(\frac{u_{\mathrm{LA}}}{\gamma_{\mathrm{d}}\chi\rho}\right)^{3/2}\min\left(1,\mathcal{M}_{\mathrm{A}}^{1/2}\right)$$

$$\approx \frac{0.0011}{L_2^{1/2}}\left(\frac{u_{\mathrm{LA},1}}{n_{\mathrm{H},3}\chi_{-4}}\right)^{3/2}\min\left(1,\mathcal{M}_{\mathrm{A}}^{1/2}\right)\ \mathrm{pc}$$

- ..much bigger than the GeV gyroradius

$$r_{\mathrm{g}} = \frac{\gamma mcv\sin\alpha}{eB} \approx \frac{E_{\mathrm{CR}}\sin\alpha}{eB} \sim 10^{-6}\ E_{\mathrm{CR},0}\ B_0^{-1}\ \mathrm{pc},$$

Implication

- The turbulence cascade in the ions cuts off at a damping scale

$$L_{\mathrm{damp,A}} = \frac{\pi}{\sqrt{2}L}\left(\frac{u_{\mathrm{LA}}}{\gamma_{\mathrm{d}}\chi\rho}\right)^{3/2}\min\left(1,\mathcal{M}_{\mathrm{A}}^{1/2}\right)$$

$$\approx \frac{0.0011}{L_2^{1/2}}\left(\frac{u_{\mathrm{LA},1}}{n_{\mathrm{H},3}\chi_{-4}}\right)^{3/2}\min\left(1,\mathcal{M}_{\mathrm{A}}^{1/2}\right)\ \mathrm{pc}$$

- ..much bigger than the GeV gyroradius

$$r_{\mathrm{g}} = \frac{\gamma mcv\sin\alpha}{eB} \approx \frac{E_{\mathrm{CR}}\sin\alpha}{eB} \sim 10^{-6}\ E_{\mathrm{CR},0}\ B_0^{-1}\ \mathrm{pc},$$

Implication

- The turbulence cascade in the ions cuts off at a damping scale

$$L_{\mathrm{damp,A}} = \frac{\pi}{\sqrt{2}L}\left(\frac{u_{\mathrm{LA}}}{\gamma_{\mathrm{d}}\chi\rho}\right)^{3/2}\min\left(1,\mathcal{M}_{\mathrm{A}}^{1/2}\right)$$

$$\approx \frac{0.0011}{L_2^{1/2}}\left(\frac{u_{\mathrm{LA},1}}{n_{\mathrm{H},3}\chi_{-4}}\right)^{3/2}\min\left(1,\mathcal{M}_{\mathrm{A}}^{1/2}\right)\ \mathrm{pc}$$

- ..much bigger than the GeV gyroradius

$$r_{\mathrm{g}} = \frac{\gamma mcv\sin\alpha}{eB} \approx \frac{E_{\mathrm{CR}}\sin\alpha}{eB} \sim 10^{-6}\ E_{\mathrm{CR},0}\ B_0^{-1}\ \mathrm{pc},$$

Implication

- The turbulence cascade in the ions cuts off at a damping scale

$$L_{\mathrm{damp,A}} = \frac{\pi}{\sqrt{2}L}\left(\frac{u_{\mathrm{LA}}}{\gamma_{\mathrm{d}}\chi\rho}\right)^{3/2}\min\left(1,\mathcal{M}_{\mathrm{A}}^{1/2}\right)$$

$$\approx \frac{0.0011}{L_2^{1/2}}\left(\frac{u_{\mathrm{LA},1}}{n_{\mathrm{H},3}\chi_{-4}}\right)^{3/2}\min\left(1,\mathcal{M}_{\mathrm{A}}^{1/2}\right)\ \mathrm{pc}$$

- ..much bigger than the GeV gyroradius

$$r_{\mathrm{g}} = \frac{\gamma mcv\sin\alpha}{eB} \approx \frac{E_{\mathrm{CR}}\sin\alpha}{eB} \sim 10^{-6}\ E_{\mathrm{CR},0}\ B_0^{-1}\ \mathrm{pc},$$

Implication

- The turbulence cascade in the ions cuts off at a damping scale

$$L_{\mathrm{damp,A}} = \frac{\pi}{\sqrt{2}L}\left(\frac{u_{\mathrm{LA}}}{\gamma_{\mathrm{d}}\chi\rho}\right)^{3/2}\min\left(1,\mathcal{M}_{\mathrm{A}}^{1/2}\right)$$

$$\approx \frac{0.0011}{L_2^{1/2}}\left(\frac{u_{\mathrm{LA},1}}{n_{\mathrm{H},3}\chi_{-4}}\right)^{3/2}\min\left(1,\mathcal{M}_{\mathrm{A}}^{1/2}\right)\ \mathrm{pc}$$

- ..much bigger than the GeV gyroradius

$$r_{\mathrm{g}} = \frac{\gamma mcv\sin\alpha}{eB} \approx \frac{E_{\mathrm{CR}}\sin\alpha}{eB} \sim 10^{-6}\ E_{\mathrm{CR},0}\ B_0^{-1}\ \mathrm{pc},$$

Implication

- The turbulence cascade in the ions cuts off at a damping scale

Alfven Mach number

$M_A \sim 2$

$$L_{\mathrm{damp,A}} = \frac{\pi}{\sqrt{2L}}\left(\frac{u_{\mathrm{LA}}}{\gamma_{\mathrm{d}}\chi\rho}\right)^{3/2}\min\left(1,\mathcal{M}_{\mathrm{A}}^{1/2}\right)$$

$$\approx \frac{0.0011}{L_2^{1/2}}\left(\frac{u_{\mathrm{LA},1}}{n_{\mathrm{H},3}\chi_{-4}}\right)^{3/2}\min\left(1,\mathcal{M}_{\mathrm{A}}^{1/2}\right)\ \mathrm{pc}$$

- ..much bigger than the GeV gyroradius

$$r_{\mathrm{g}} = \frac{\gamma mcv\sin\alpha}{eB} \approx \frac{E_{\mathrm{CR}}\sin\alpha}{eB} \sim 10^{-6}\ E_{\mathrm{CR},0}\ B_0^{-1}\ \mathrm{pc},$$

Implication

- Thus, GeV CRs can***not*** scatter off the strong, large-scale turbulence found in starbursts, because efficient ion-neutral damping prevents such turbulence from cascading down to their ~10^{-6} pc gyroradius scale
- Instead, GeV CRs stream along field lines at a rate determined by the **competition between streaming instability and ion-neutral damping; *self-excited turbulence*.**
- Unless the CR number density is small, the streaming speed works out to be very close to the ***ion*** Alfven speed, V_{Ai}

Implication

- No source of turbulence on the CR gyroscale other than that excited by the streaming instability
- ⇒ no mechanism to scatter CRs perpendicular to field lines.
- ⇒ diffusion relative to the macroscopic mean magnetic field direction is solely due to **field line random walk** (**FLRW**)

Implication

- The diffusion rate due to this process is determined by the streaming speed and the **coherence length of the field L_A,** which is related to the injection length of the turbulence L by (Yan & Lazarian (2008):

$$L_A \simeq \frac{L}{M_A^3} \quad ; \quad M_A > 1$$

- Can now estimate the effective macroscopic diffusion coefficient (Yan & Lazarian 2008) for CRs in the direction parallel to the large-scale field:

$$D_{\parallel} \approx V_{\rm st} L_{\rm A}$$

- Can now estimate the effective macroscopic diffusion coefficient (Yan & Lazarian 2008) for CRs in the direction parallel to the large-scale field:

$$D_{\parallel} \approx V_{\rm st} L_{\rm A}$$

- If $M_A > 1$ as expected, then the perturbations in the field are not preferentially aligned with the large-scale mean field, and thus the diffusion coefficient perpendicular to the large-scale field is the same as that parallel to it and thus there is **a single diffusion coefficient D in all directions:** $D_\perp \approx D_\parallel$

- Can now estimate the effective macroscopic diffusion coefficient (Yan & Lazarian 2008) for CRs in the direction parallel to the large-scale field:

$$D_{\parallel} \approx V_{\rm st} L_{\rm A}$$
$$\approx 3.1 \times 10^{28} \frac{u_{\rm LA,1} L_2}{\sqrt{\chi - 4}} \min\left(\mathcal{M}_{\rm A}^{-1}, \mathcal{M}_{\rm A}^{-4}\right) \ {\rm cm}^2 \ {\rm s}^{-1},$$

- If $M_A > 1$ as expected, then the perturbations in the field are not preferentially aligned with the large-scale mean field, and thus the diffusion coefficient perpendicular to the large-scale field is the same as that parallel to it and thus there is **a single diffusion coefficient D in all directions:** $D_\perp \approx D_\parallel$

- Note D is energy independent AND similar in magnitude to Galactic value @ ~10 GeV

- Can now estimate the effective macroscopic diffusion coefficient (Yan & Lazarian 2008) for CRs in the direction parallel to the large-scale field:

$$D_{\parallel} \approx V_{\rm st} L_{\rm A}$$
$$\approx 3.1 \times 10^{28} \frac{v_{\rm LA,1} L_2}{\sqrt{\chi - 4}} \min\left(\mathcal{M}_{\rm A}^{-1}, \mathcal{M}_{\rm A}^{-4}\right) \ {\rm cm}^2 \ {\rm s}^{-1},$$

- If $M_A > 1$ as expected, then the perturbations in the field are not preferentially aligned with the large-scale mean field, and thus the diffusion coefficient perpendicular to the large-scale field is the same as that parallel to it and thus there is **a single diffusion coefficient D in all directions:** $D_\perp \approx D_\parallel$

- Note D is energy independent AND similar in magnitude to Galactic value @ ~10 GeV

Application I: Starburst Gamma-Ray Spectra

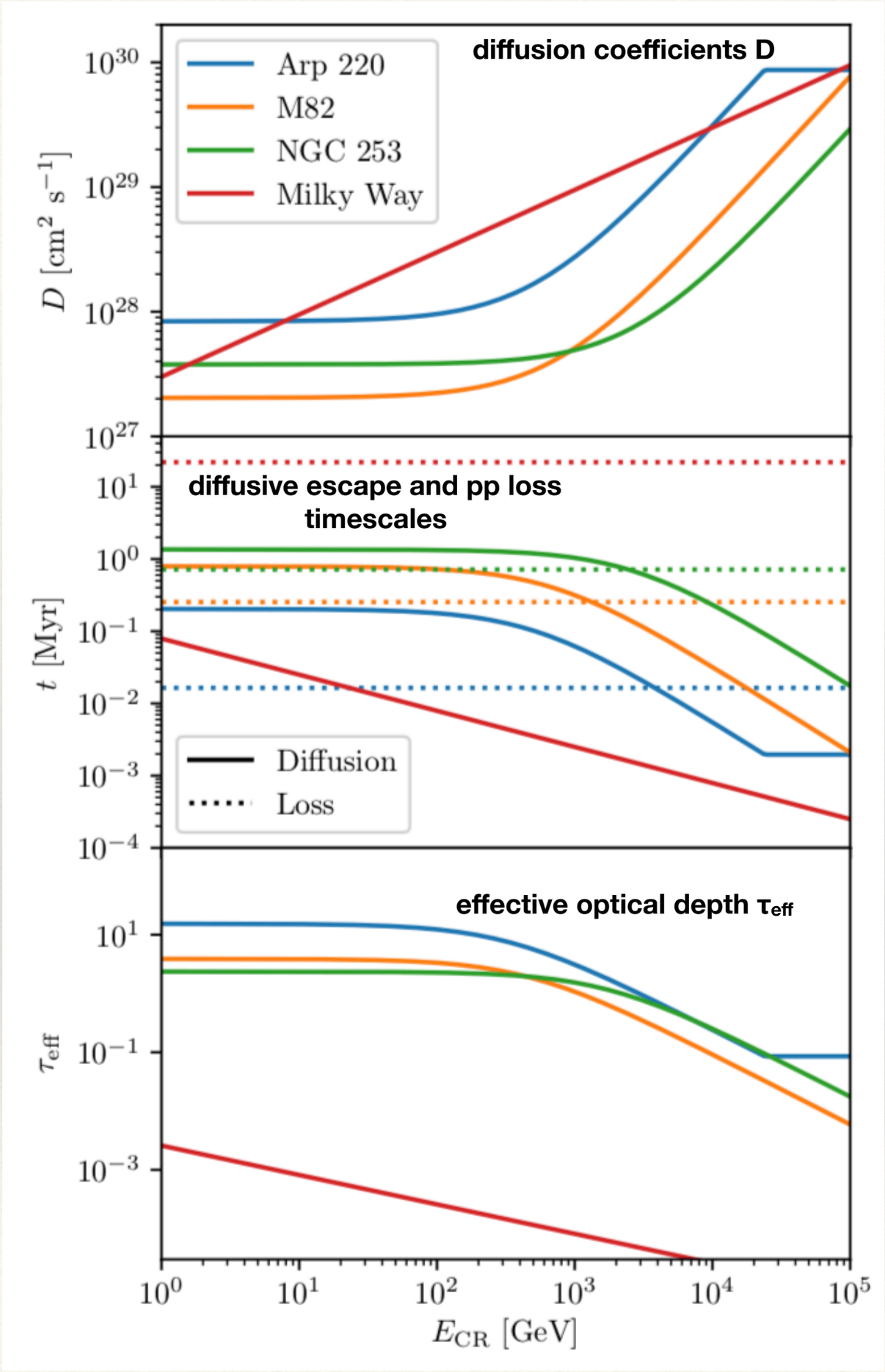

$$
\begin{aligned}
D_{\parallel} &\approx V_{\rm st} L_{\rm A} \\
&\approx 3.1 \times 10^{28} \frac{u_{\rm LA,1} L_2}{\sqrt{\chi_{-4}}} \min\left(\mathcal{M}_{\rm A}^{-1}, \mathcal{M}_{\rm A}^{-4}\right) \ {\rm cm}^2 \ {\rm s}^{-1},
\end{aligned}
$$

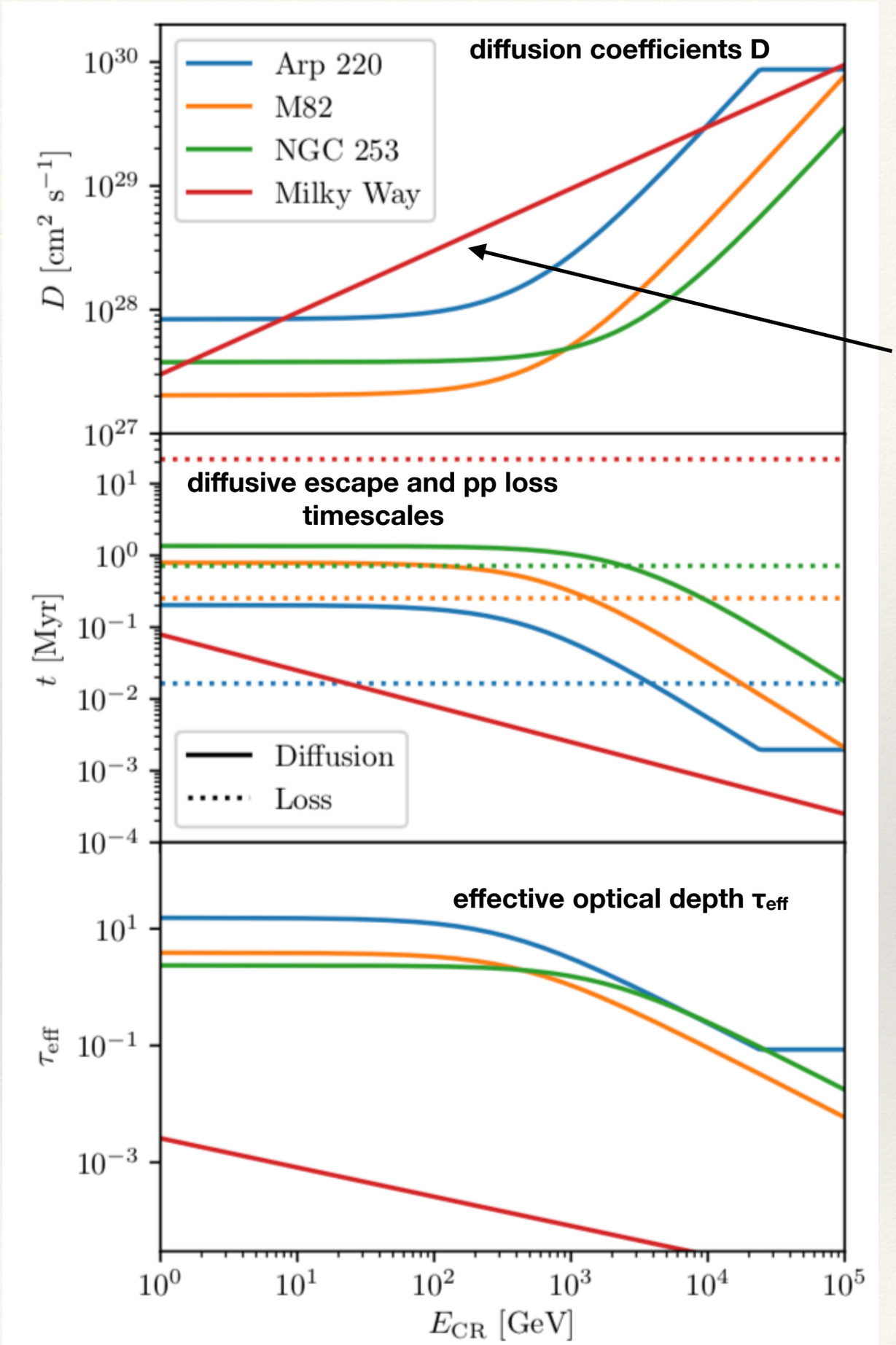

$$D_{\parallel} \approx V_{\rm st} L_{\rm A}$$
$$\approx 3.1 \times 10^{28} \frac{u_{\rm LA,1} L_2}{\sqrt{\chi_{-4}}} \min\left(\mathcal{M}_{\rm A}^{-1}, \mathcal{M}_{\rm A}^{-4}\right) \ {\rm cm}^2 \ {\rm s}^{-1},$$

$$D_{\rm MW} \approx 3 \times 10^{27} E_{\rm CR,0}^{1/2} \ {\rm cm}^2 \ {\rm s}^{-1}$$

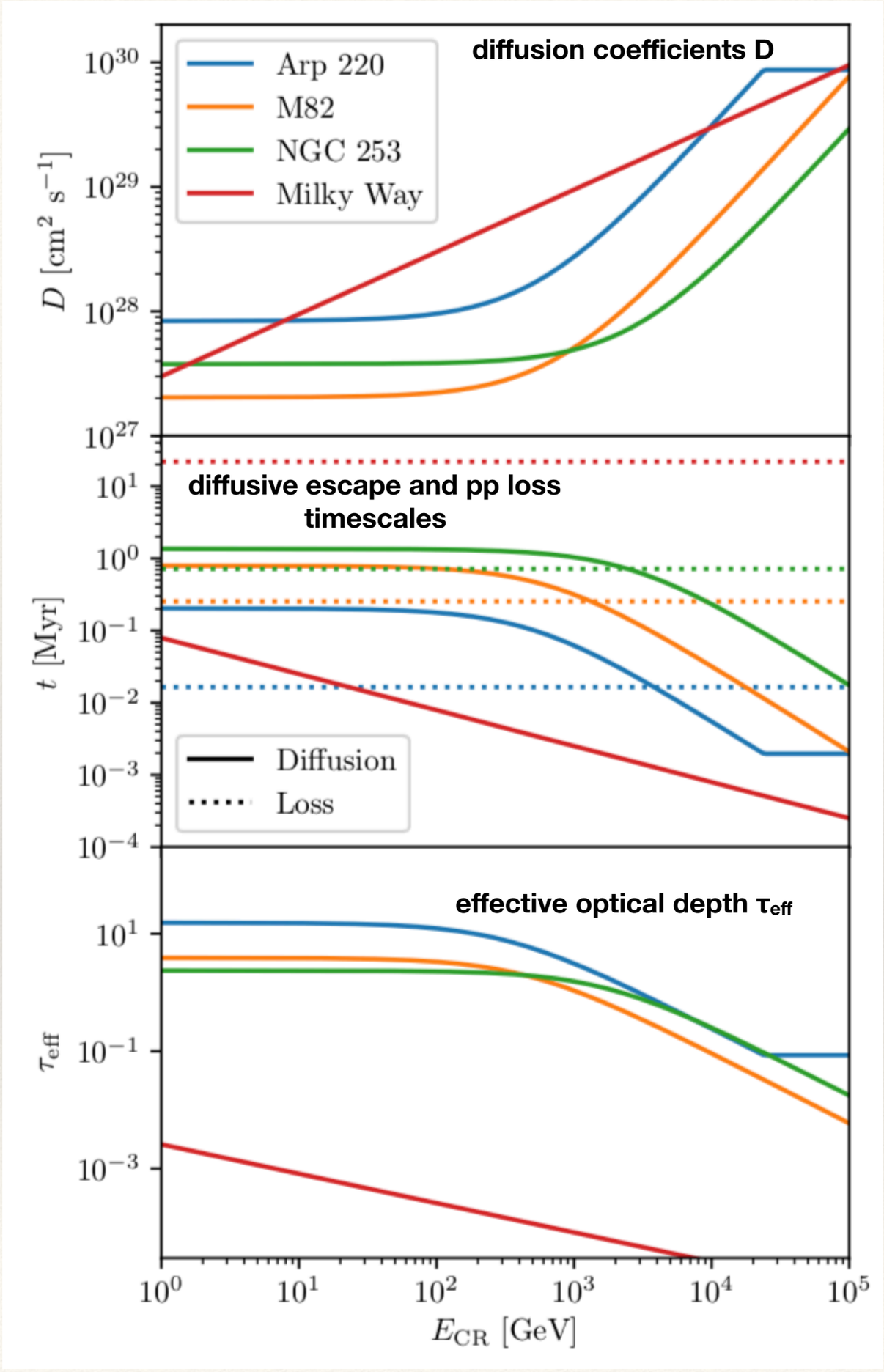

$$
\begin{aligned}
D_{\parallel} &\approx V_{\rm st} L_{\rm A} \\
&\approx 3.1 \times 10^{28} \frac{u_{\rm LA,1} L_2}{\sqrt{\chi_{-4}}} \min\left(\mathcal{M}_{\rm A}^{-1}, \mathcal{M}_{\rm A}^{-4}\right) \ {\rm cm}^2 \ {\rm s}^{-1},
\end{aligned}
$$

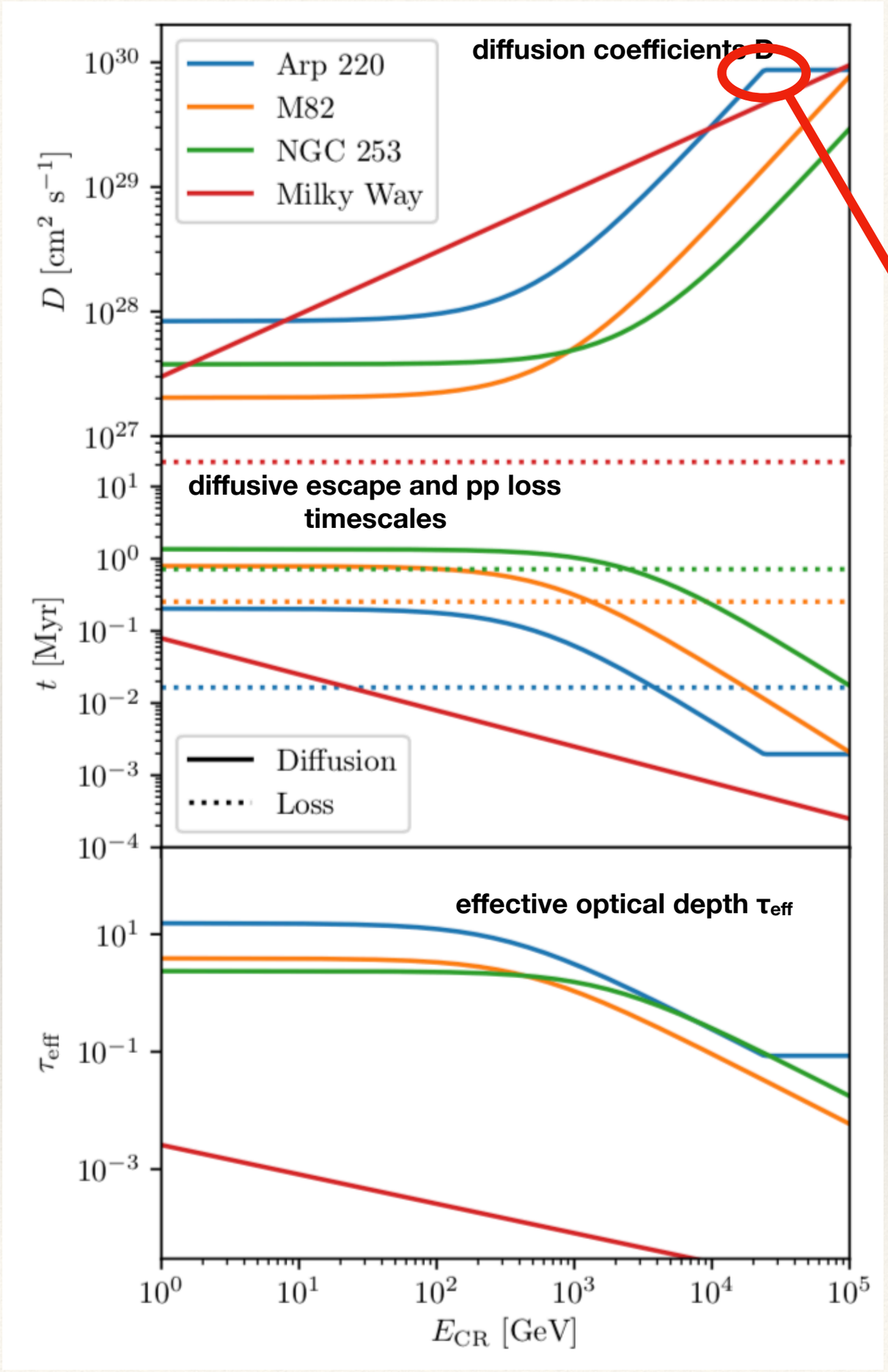

$$D_{\parallel} \approx V_{\rm st} L_{\rm A} \approx 3.1 \times 10^{28} \frac{u_{\rm LA,1} L_2}{\sqrt{\chi_{-4}}} \min\left(\mathcal{M}_{\rm A}^{-1}, \mathcal{M}_{\rm A}^{-4}\right) \ {\rm cm}^2 \ {\rm s}^{-1},$$

CR streaming speed approaches c

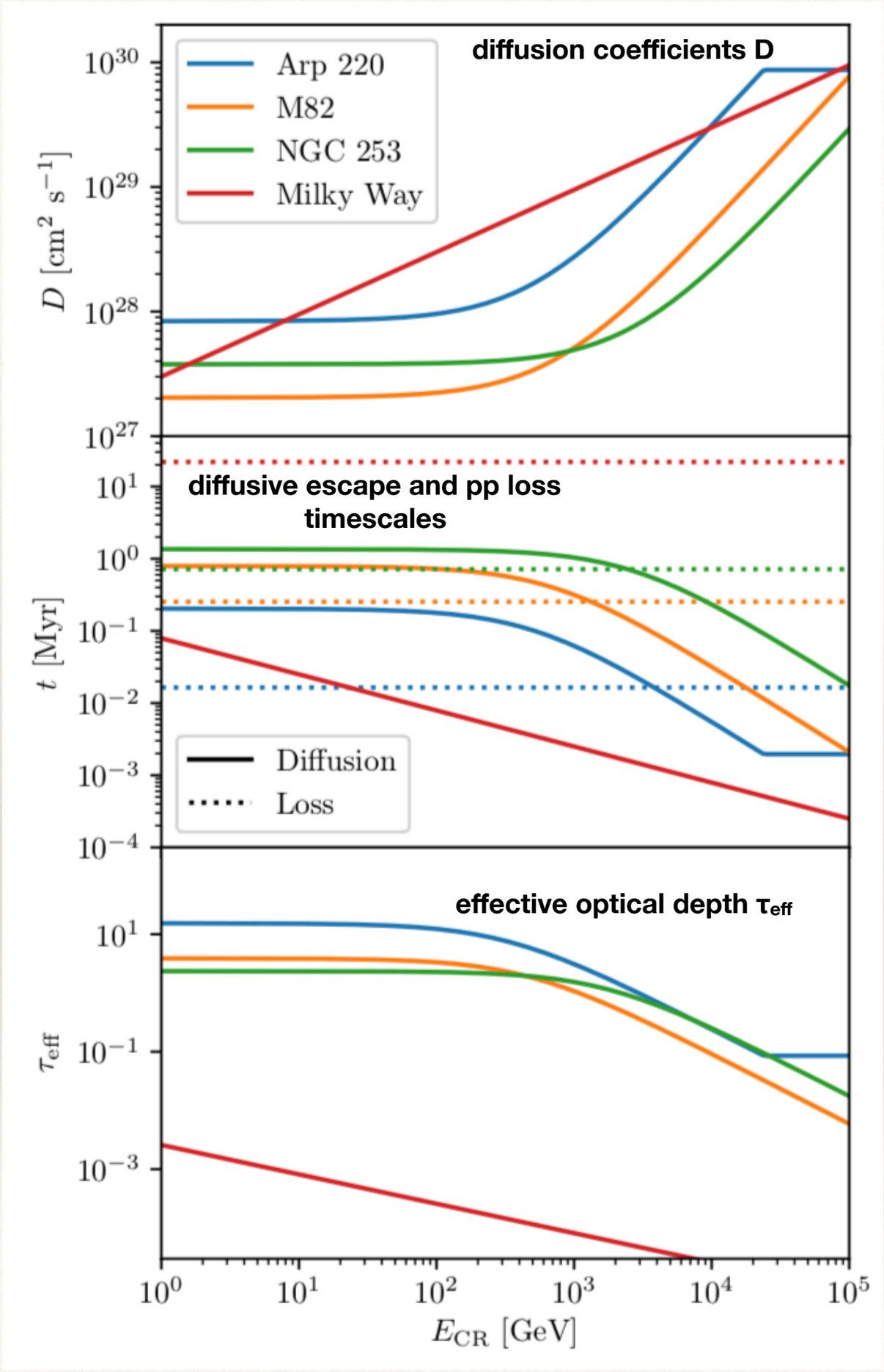

$$D_{\parallel} \approx V_{\rm st} L_{\rm A}$$

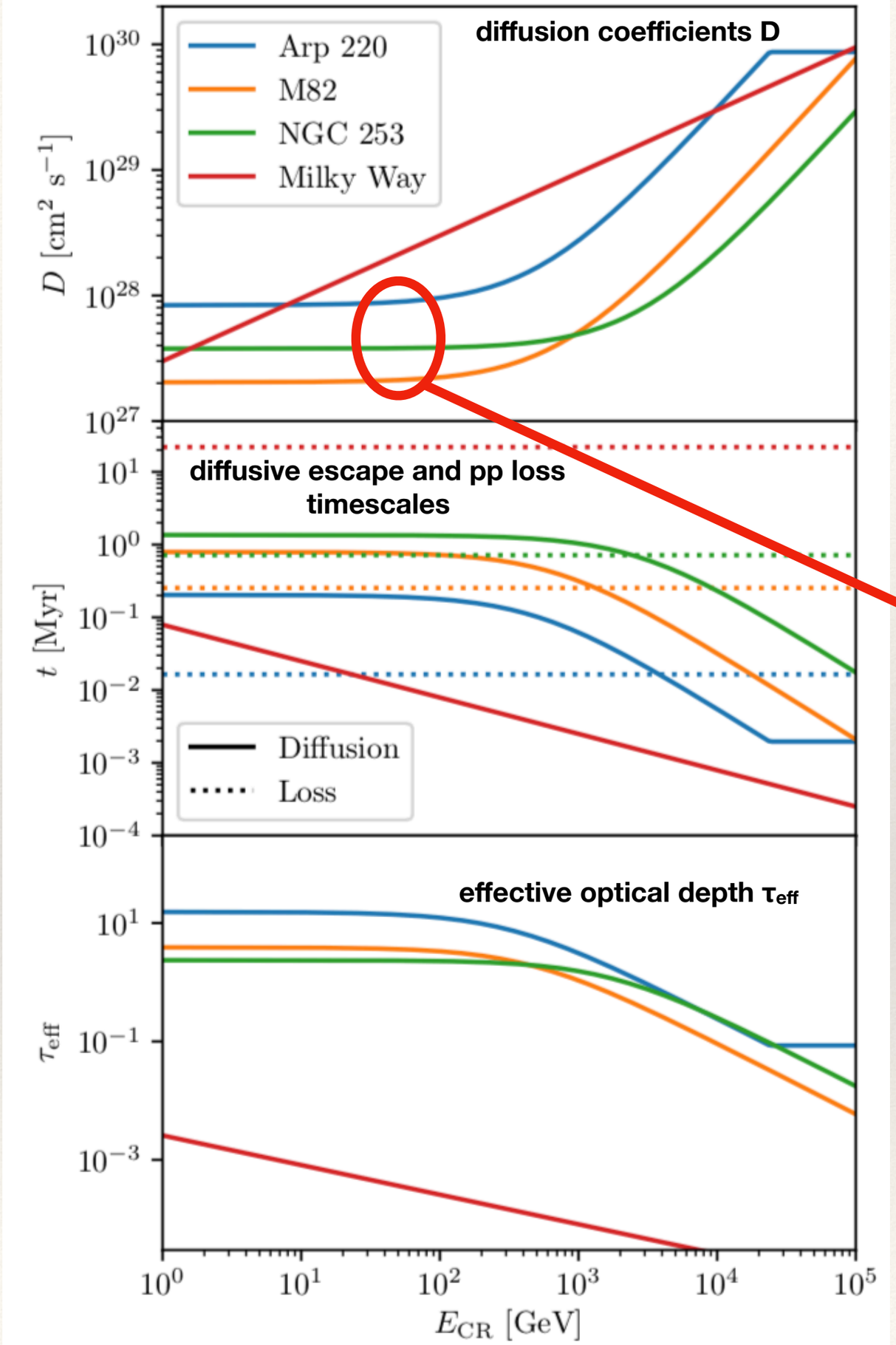

$$D_{\parallel} \approx V_{\rm st} L_{\rm A}$$

Note energy-independent D here;

Other models invoke energy-independent wind advection here at v_{wind} ~ 500 km/s, but the molecular gas in SBs is NOT advected at this speed

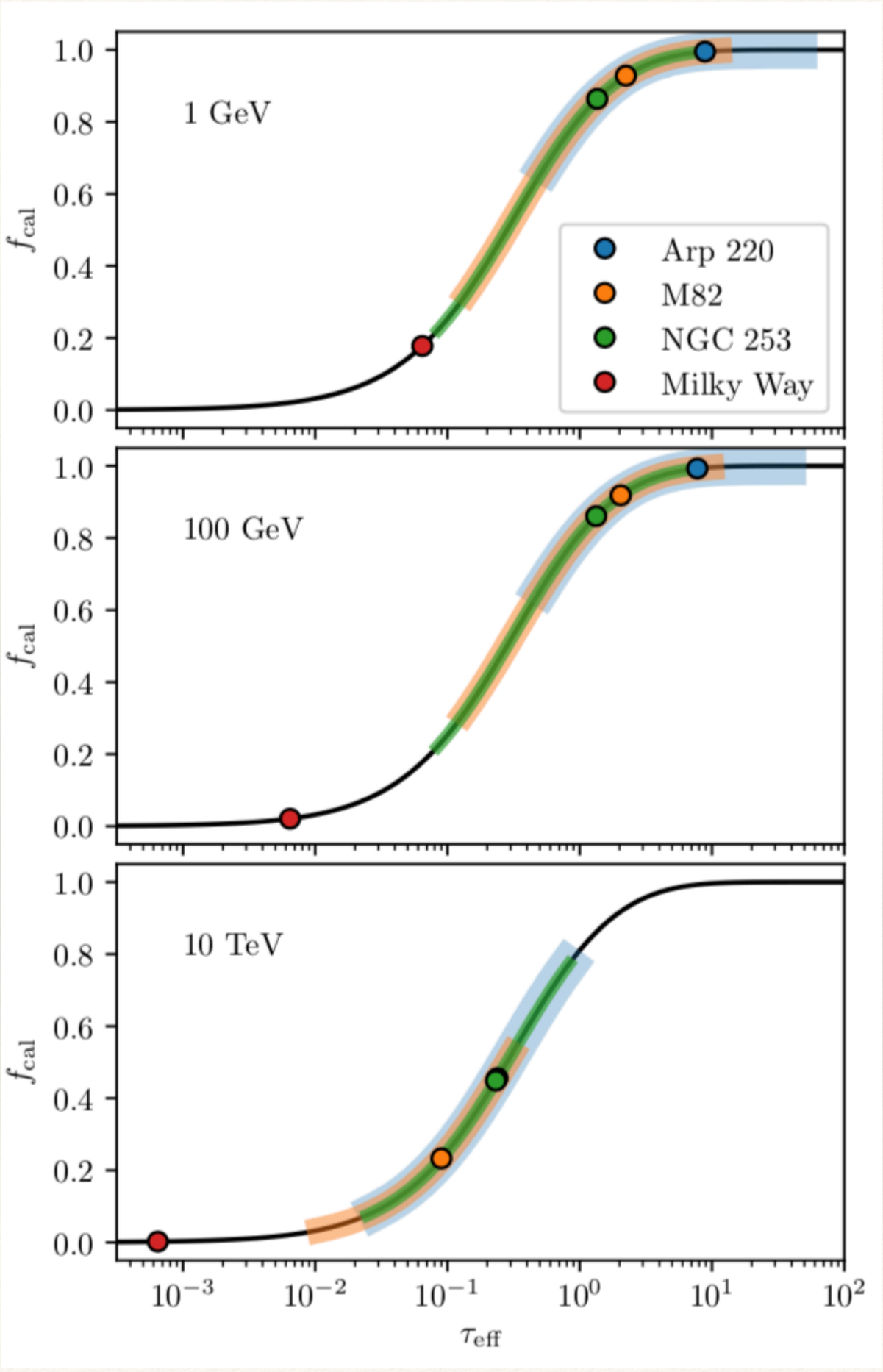

Calorimetric fraction f_{cal} as a function of effective optical depth τ_{eff}

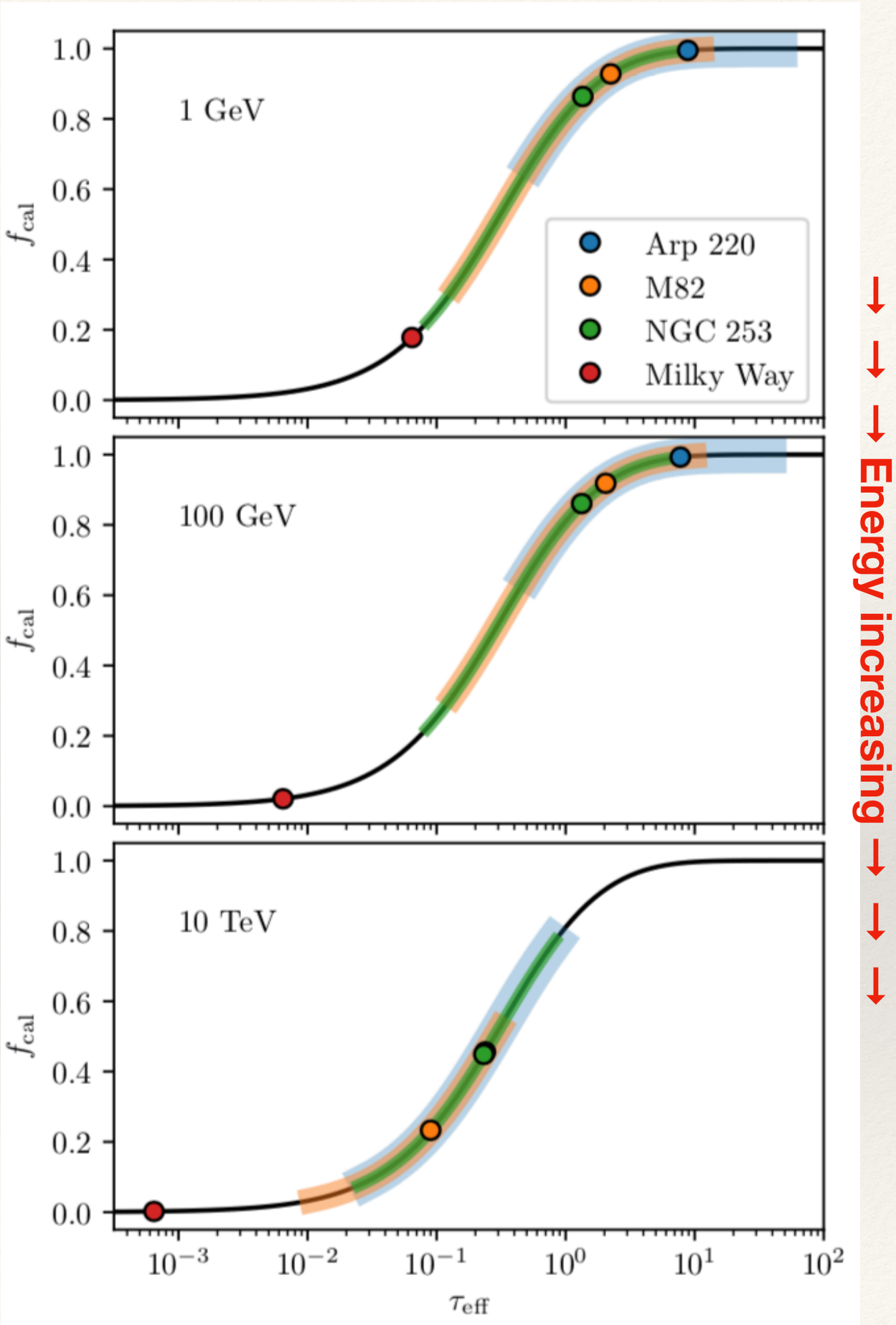

↓ ↓ ↓ Energy increasing ↓ ↓ ↓ ↓

Calorimetric fraction f_{cal} as a function of effective optical depth τ_{eff}

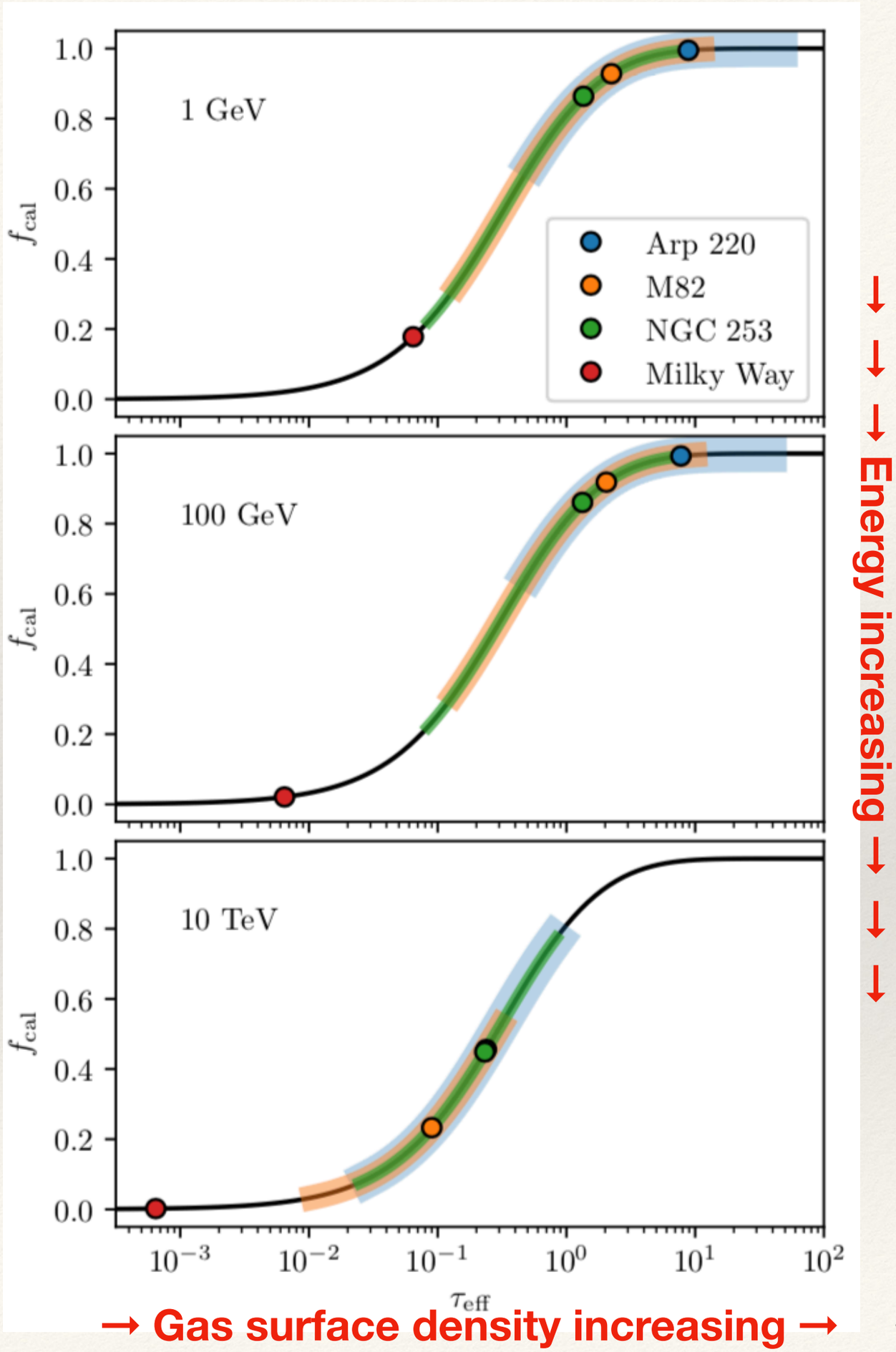

Calorimetric fraction f_{cal} as a function of effective optical depth τ_{eff}

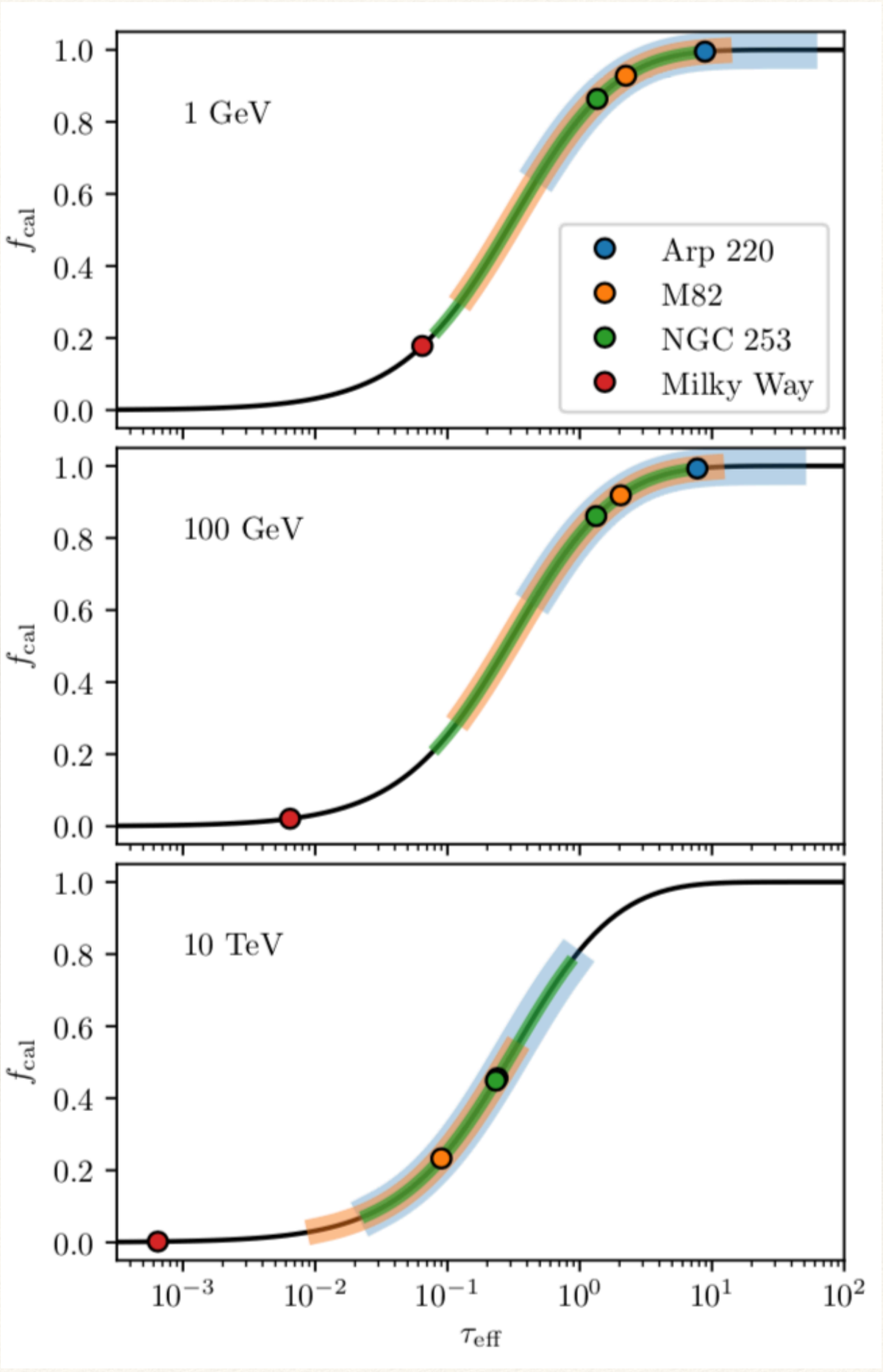

Calorimetric fraction f_{cal} as a function of effective optical depth τ_{eff}

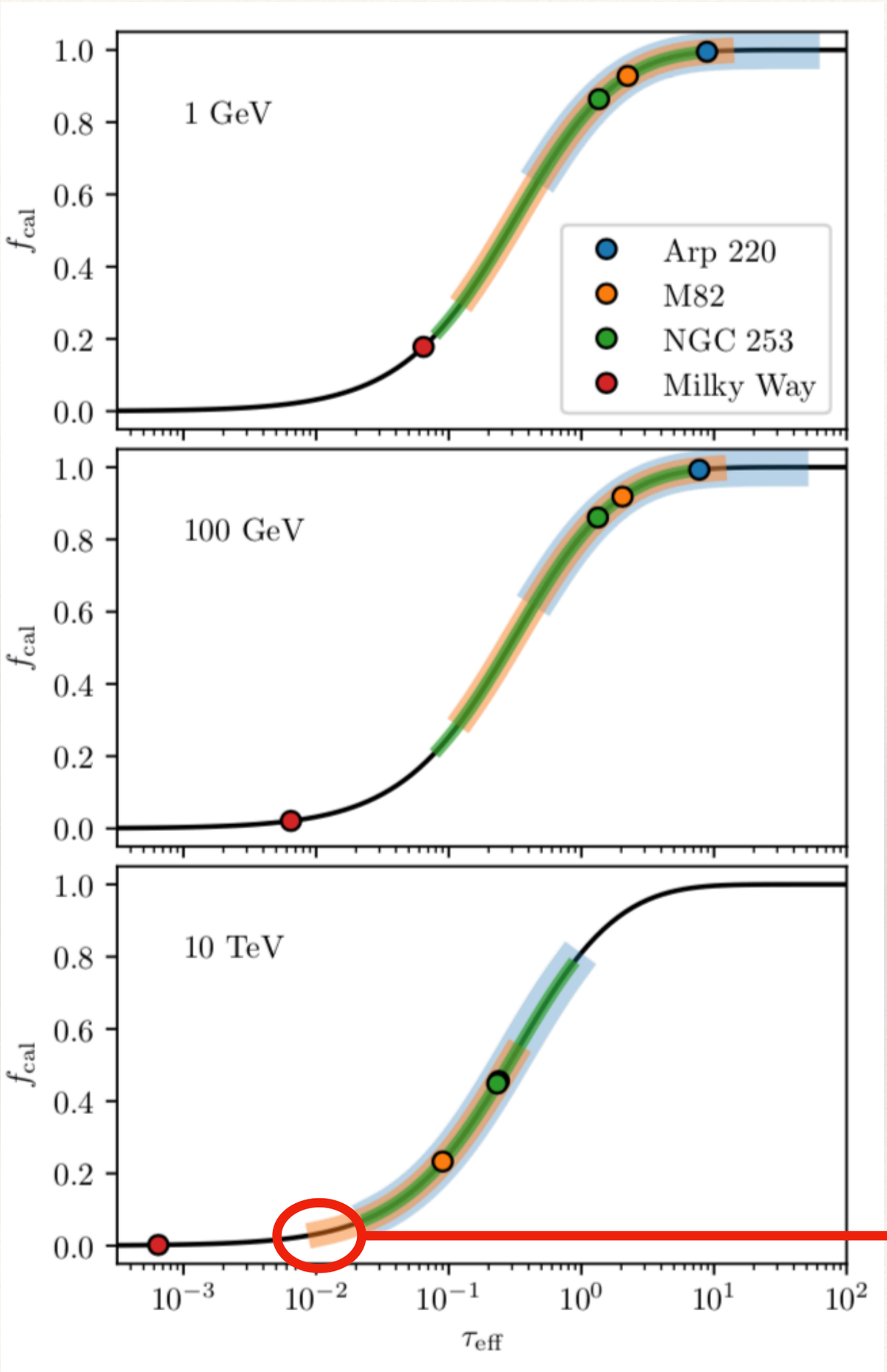

Calorimetric fraction f_{cal} as a function of effective optical depth τ_{eff}

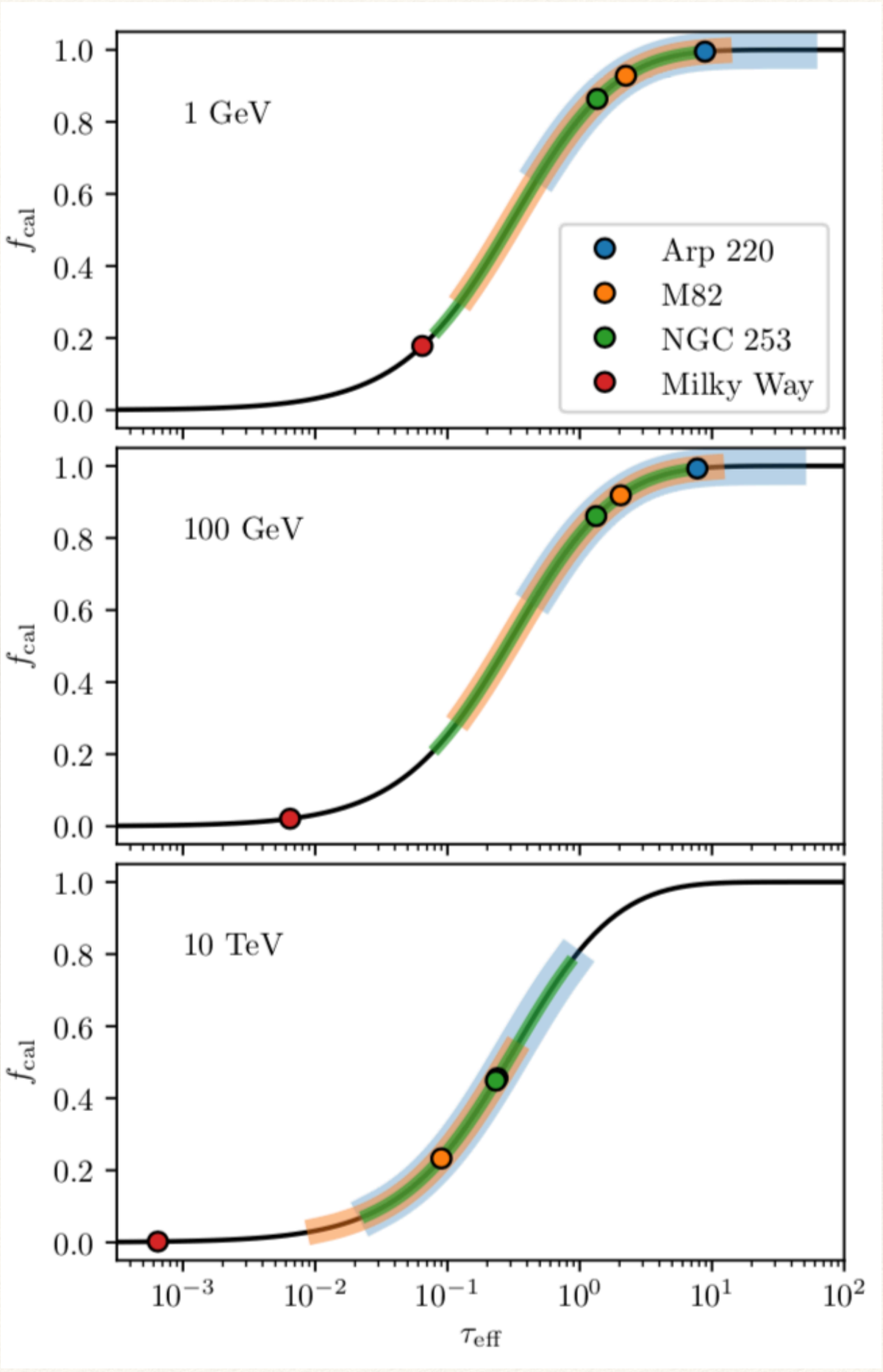

Calorimetric fraction f_{cal} as a function of effective optical depth τ_{eff}

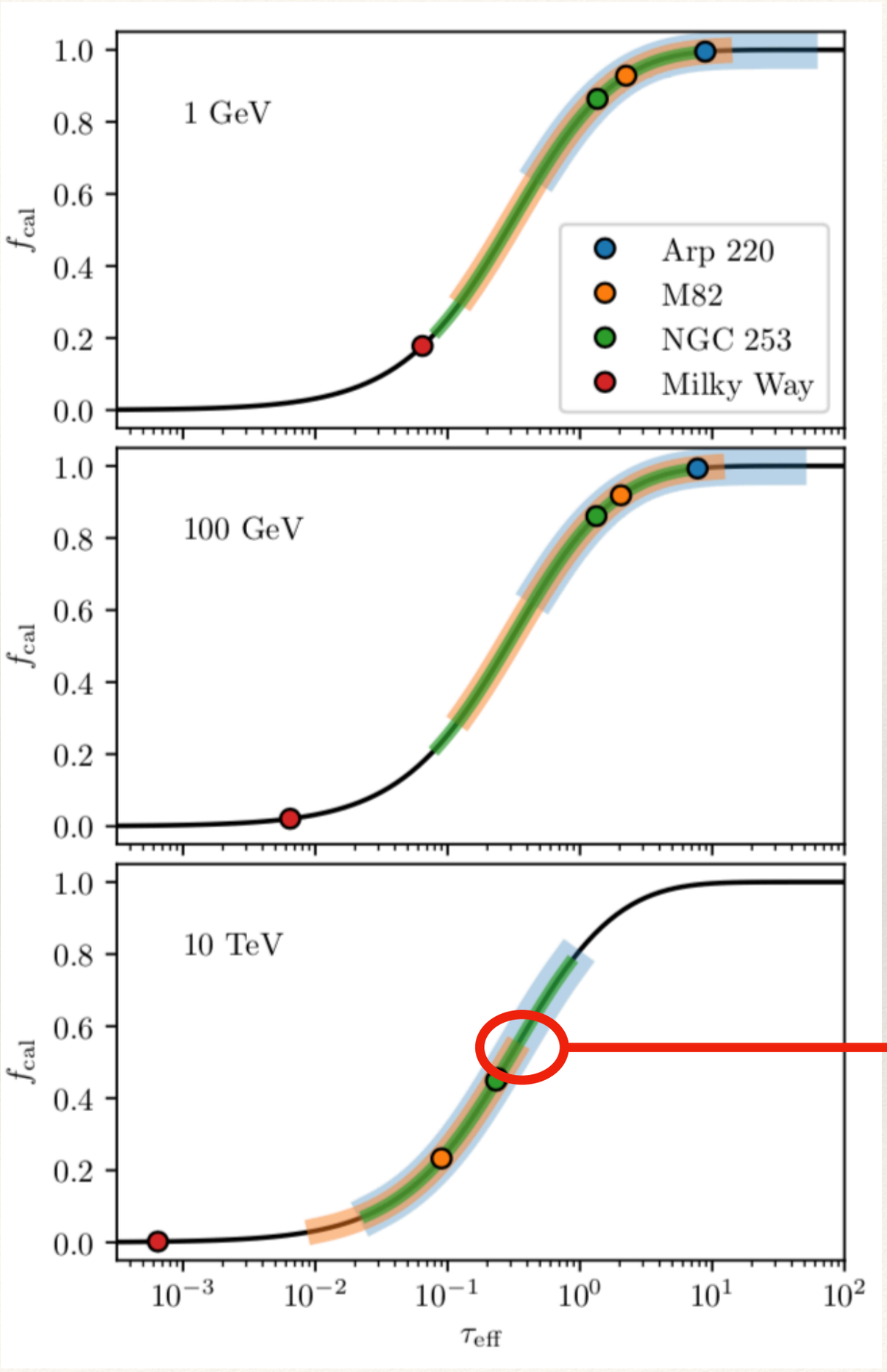

Calorimetric fraction f_{cal} as a function of effective optical depth τ_{eff}

M_A = 3

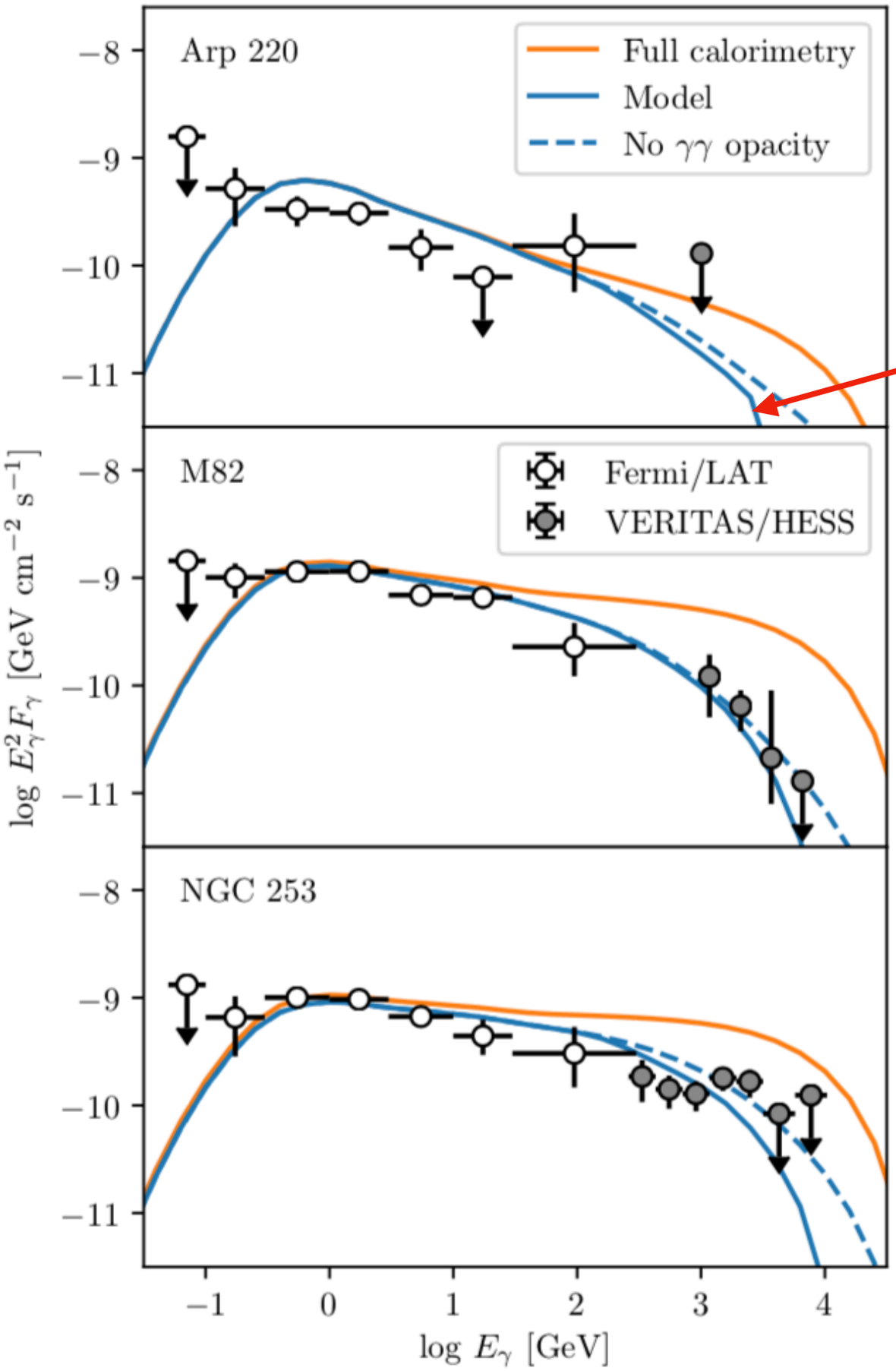

Spectra of NGC 253, M82, and Arp 220

Solid blue lines: standard model

dashed blue lines: predictions if we ignore the effects of $\gamma\gamma$ opacity

orange lines: spectra expected for perfect calorimetry independent of CR energy.

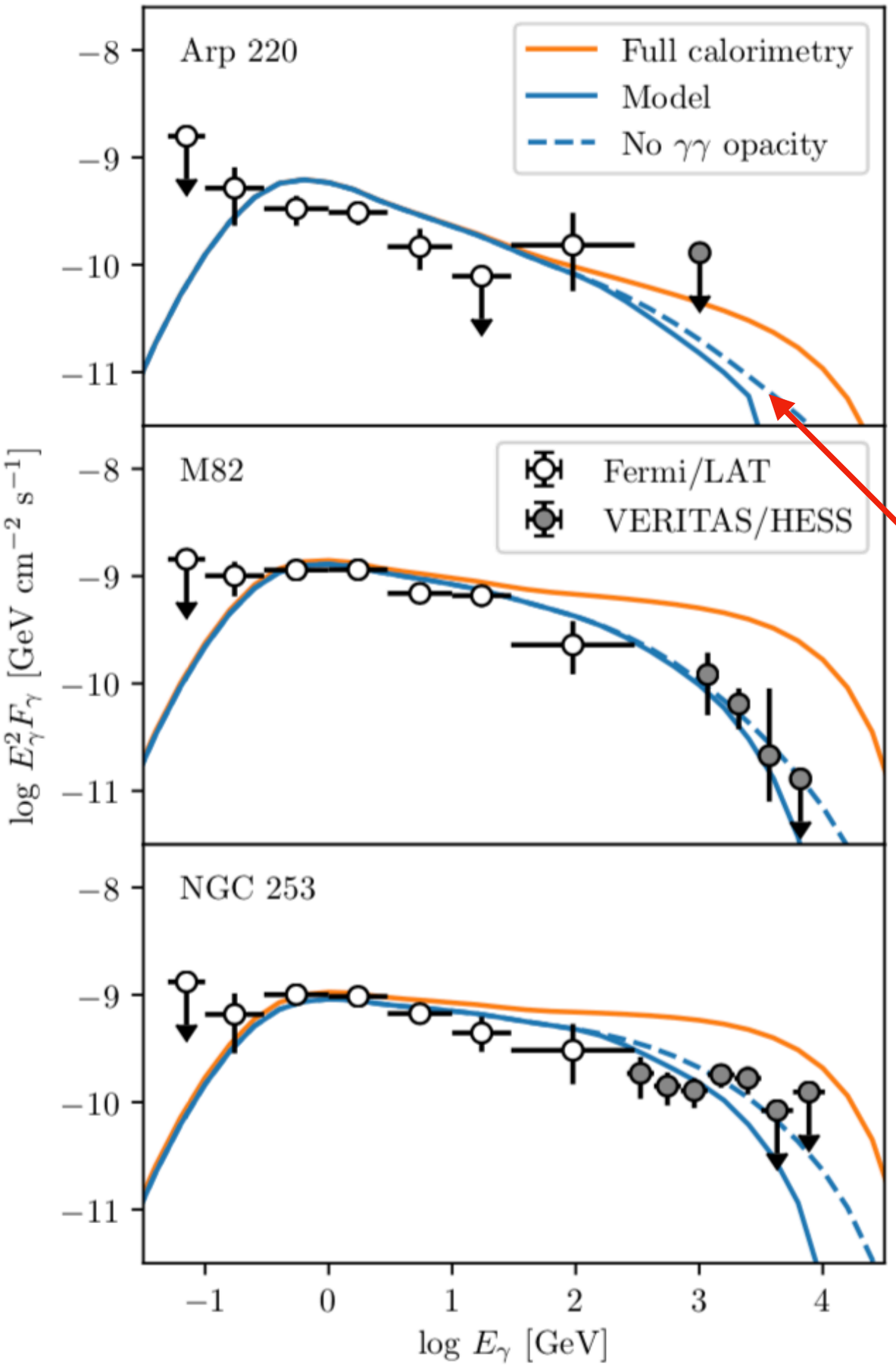

Spectra of NGC 253, M82, and Arp 220

Solid blue lines: standard model

dashed blue lines: predictions if we ignore the effects of $\gamma\gamma$ opacity

orange lines: spectra expected for perfect calorimetry independent of CR energy.

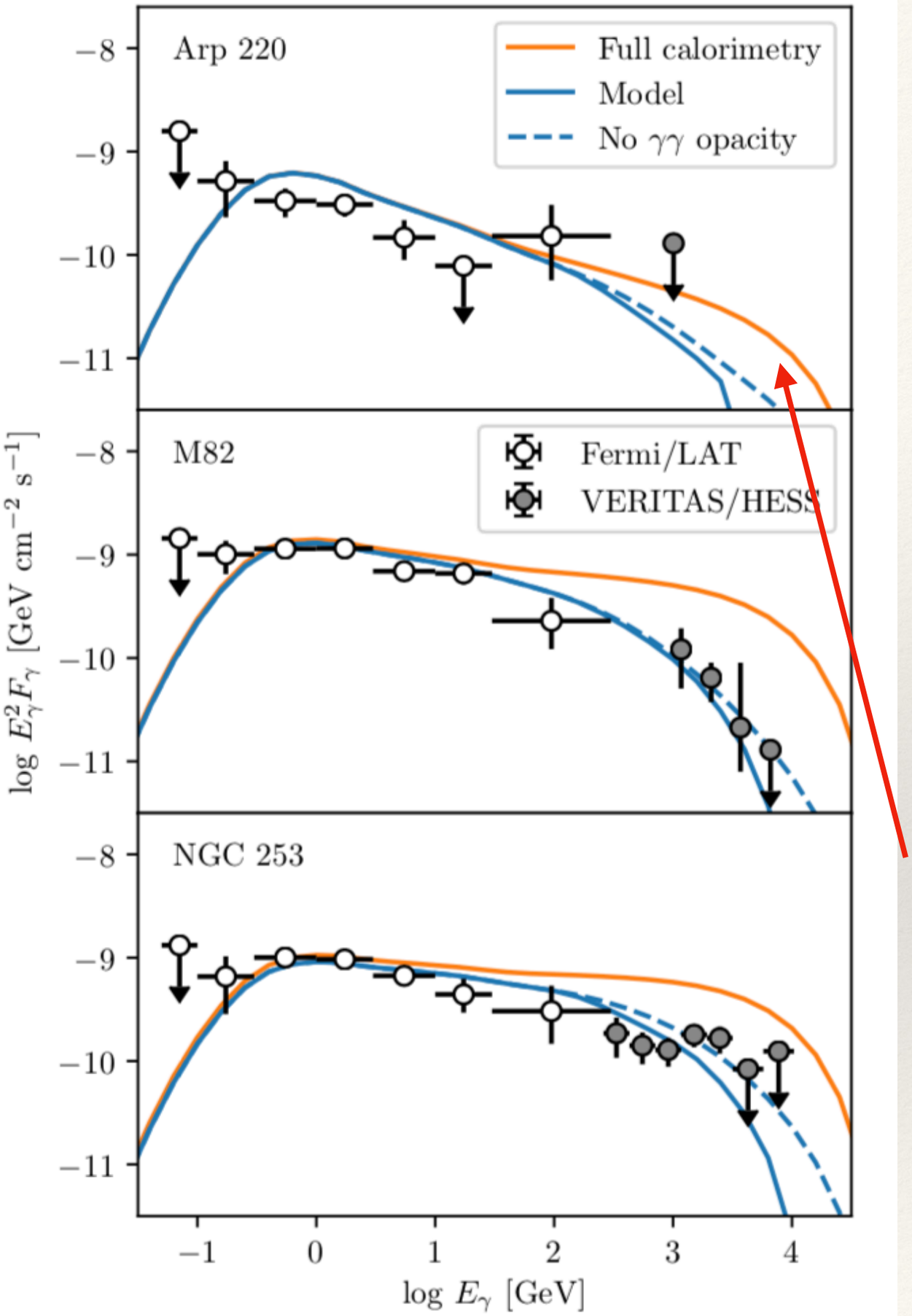

Spectra of NGC 253, M82, and Arp 220

Solid blue lines: standard model

dashed blue lines: predictions if we ignore the effects of $\gamma\gamma$ opacity

orange lines: spectra expected for perfect calorimetry independent of CR energy.

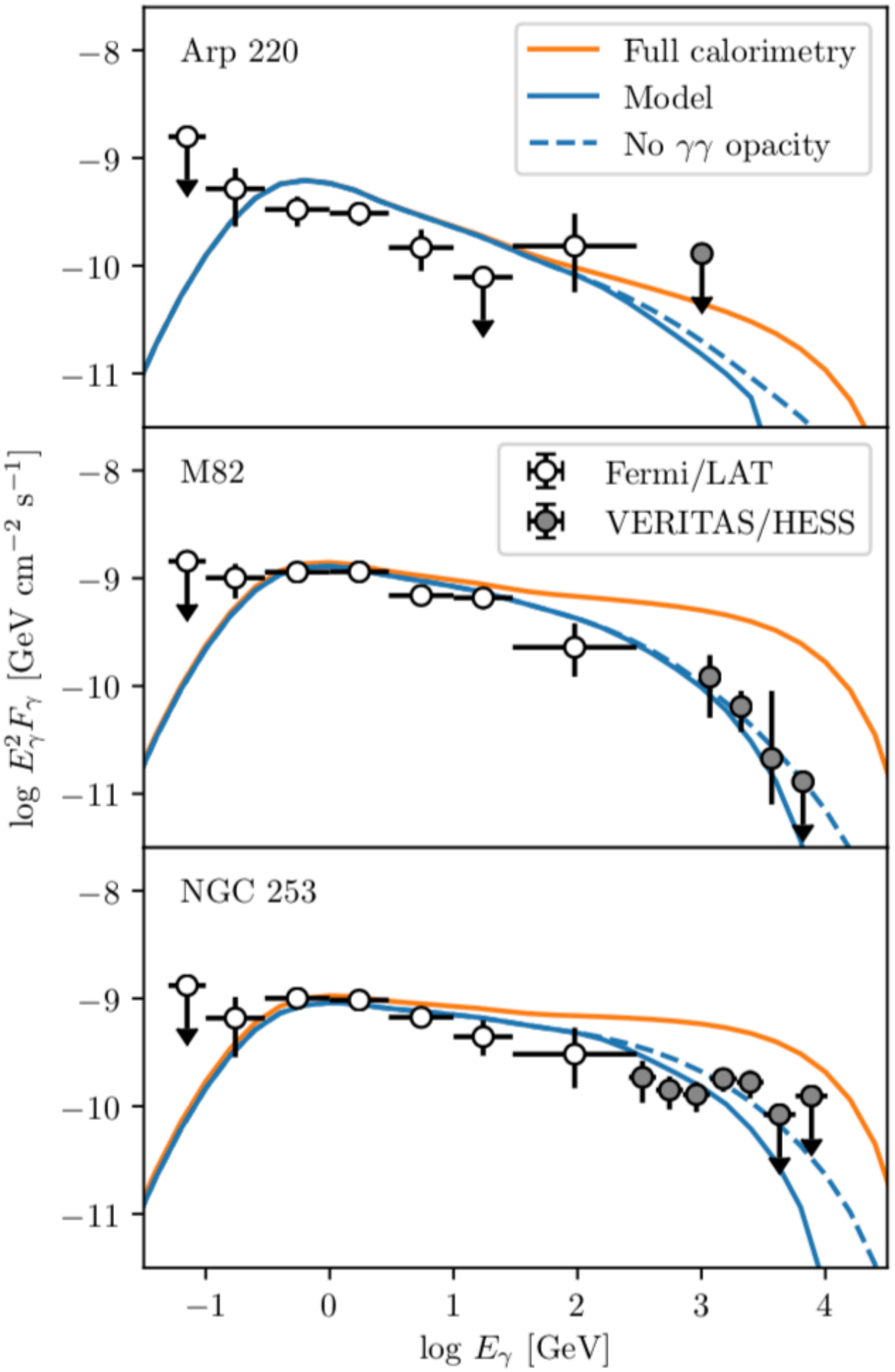

Spectra of NGC 253, M82, and Arp 220

Solid blue lines: standard model

dashed blue lines: predictions if we ignore the effects of $\gamma\gamma$ opacity

orange lines: spectra expected for perfect calorimetry independent of CR energy.

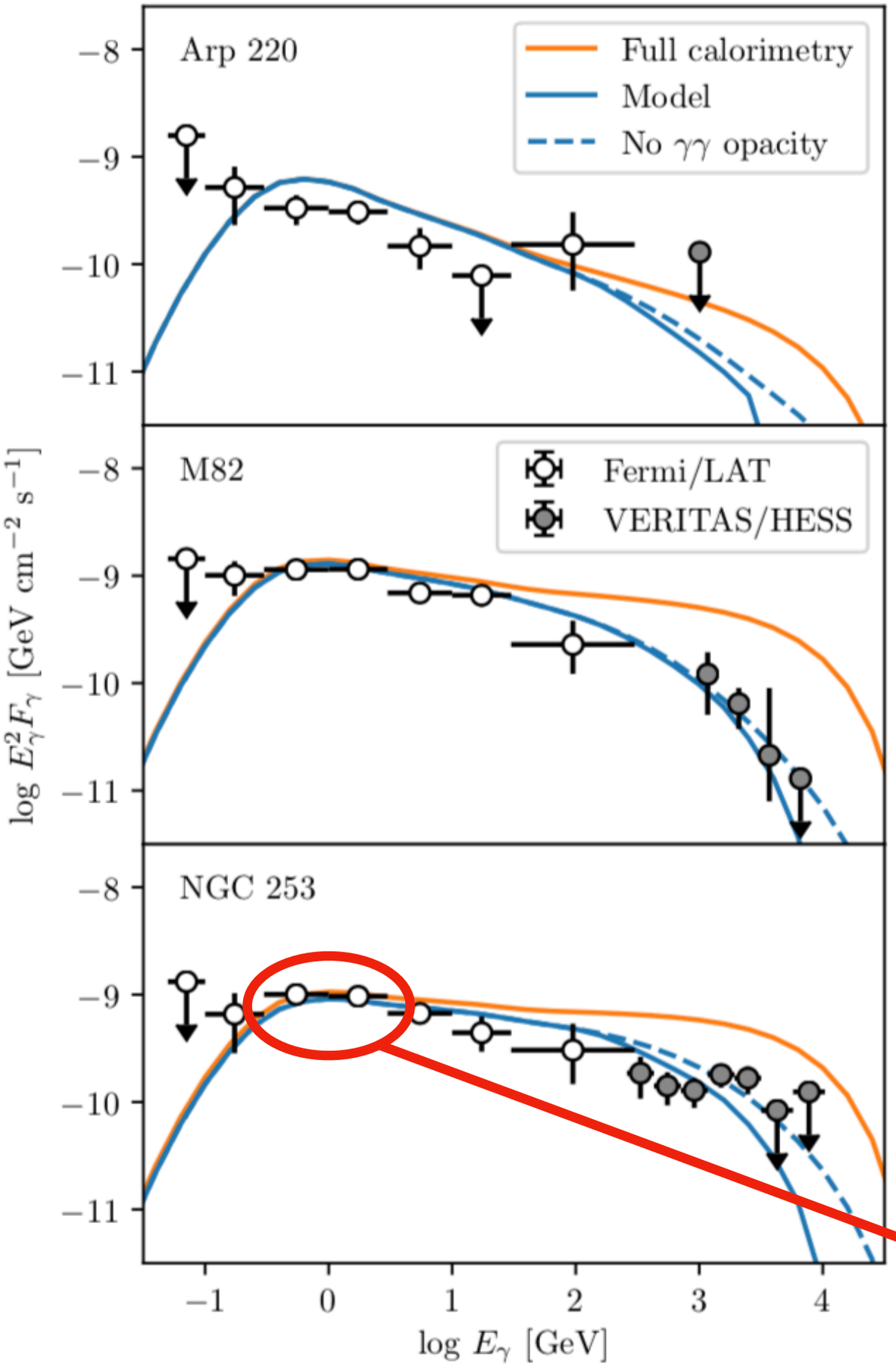

Spectra of NGC 253, M82, and Arp 220

Solid blue lines: standard model

dashed blue lines: predictions if we ignore the effects of $\gamma\gamma$ opacity

orange lines: spectra expected for perfect calorimetry independent of CR energy.

Spectral index from *Fermi* ~GeV data

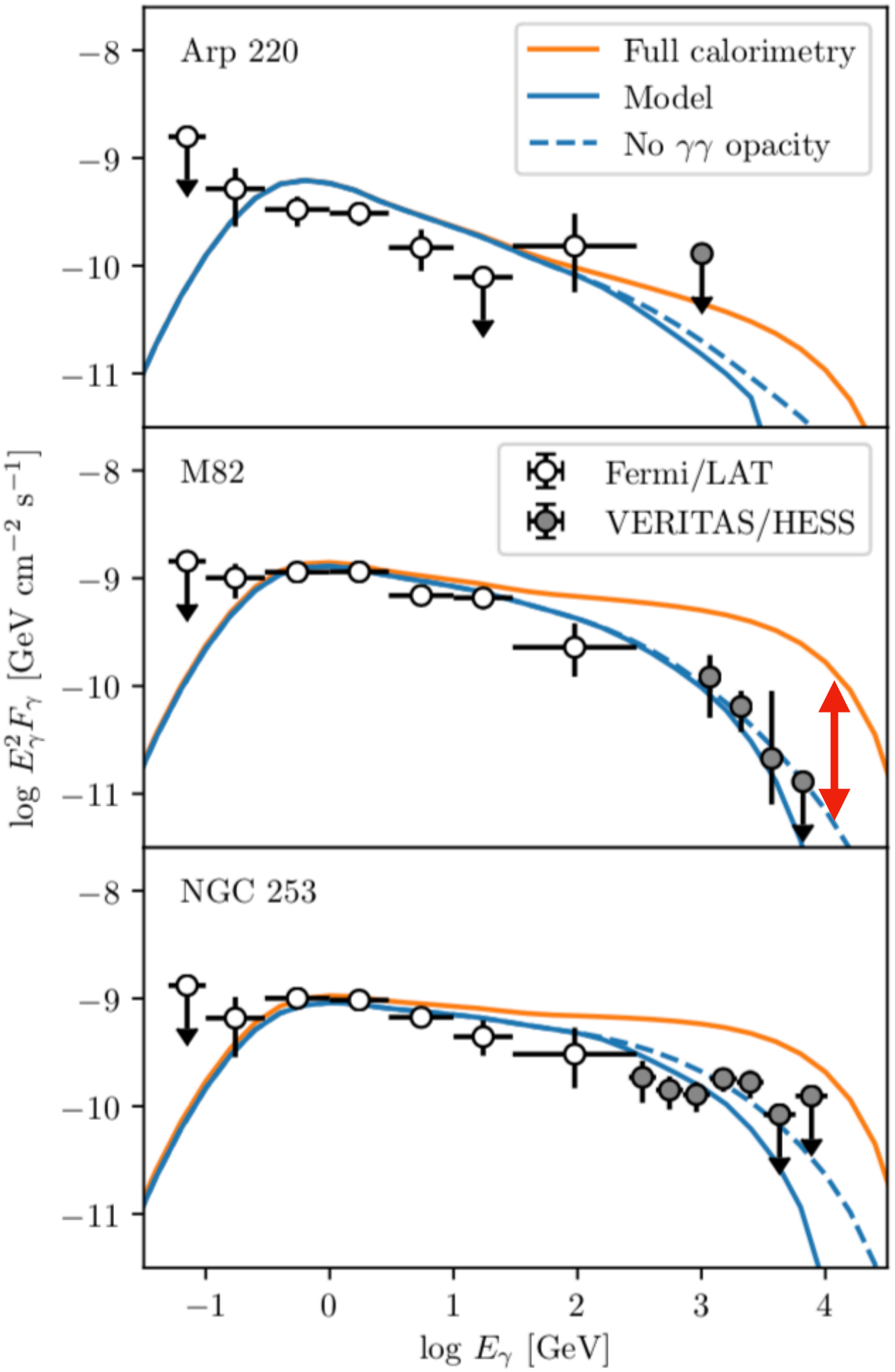

Spectra of NGC 253, M82, and Arp 220

Solid blue lines: standard model

dashed blue lines: predictions if we ignore the effects of $\gamma\gamma$ opacity

orange lines: spectra expected for perfect calorimetry independent of CR energy.

Application II: Cosmic Ray Feedback in 'Normal' Galaxies

Star-forming Galaxies; Kennicutt-Schmidt Plane

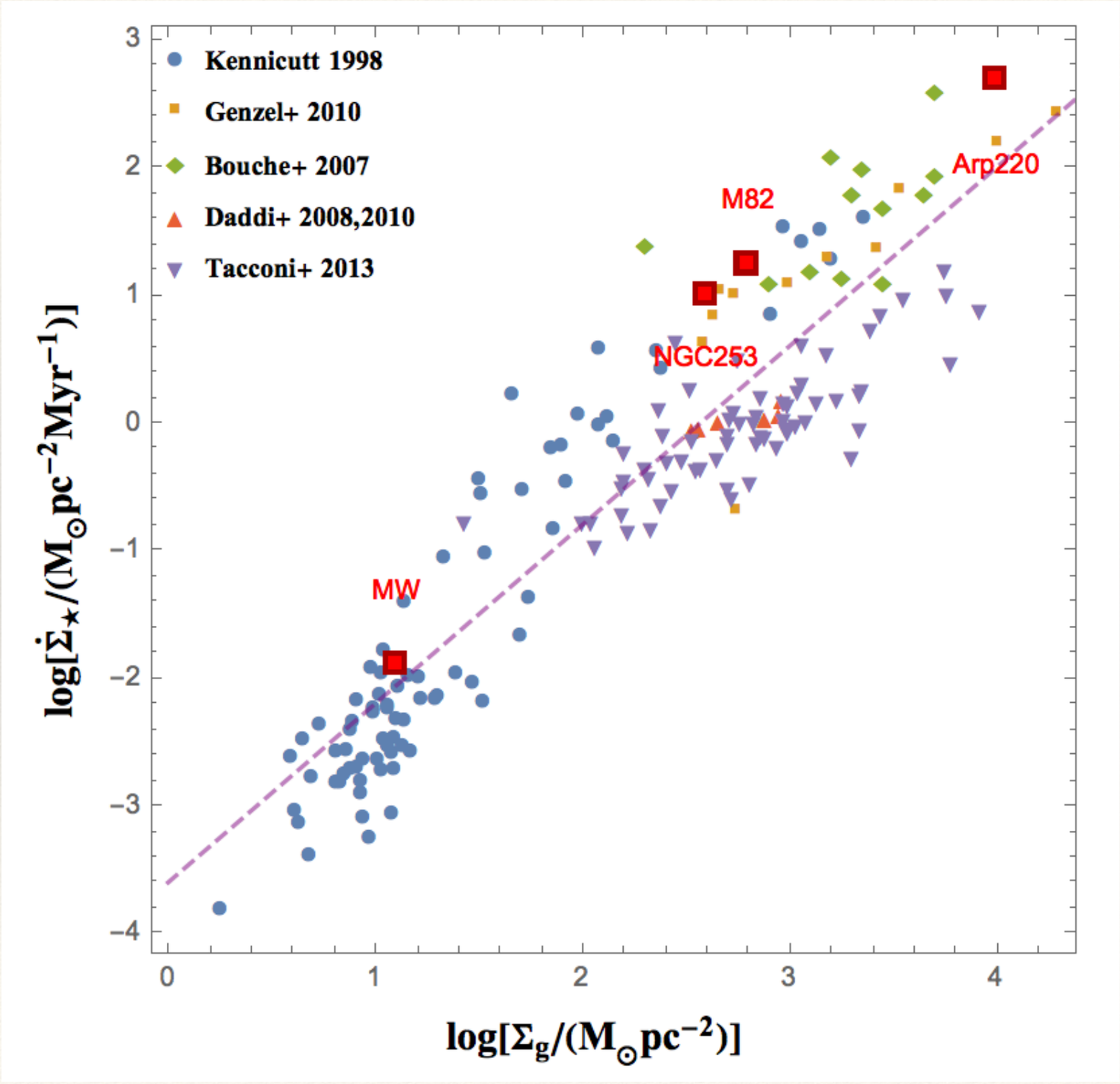

Coupled ODEs:

$$\frac{d}{d\xi}\left[-\left(\frac{ds}{d\xi}\right)^{-\beta}\frac{dp_c}{d\xi}\right] = 4{\tau_s}^2\left(\frac{ds}{d\xi}\right)^{\beta} p_c - \tau_{\text{path}}\frac{ds}{d\xi}p_c + \tau_s\frac{dp_c}{d\xi}$$

$$\frac{dp_c}{d\xi} + \xi_{\text{turb}}\frac{d^2s}{d\xi^2} = -\left(1 - f_{\text{gas}}\right)\frac{ds}{d\xi} - f_{\text{gas}}s\frac{ds}{d\xi}$$

Coupled ODEs:

$$\frac{d}{d\xi}\left[-\left(\frac{ds}{d\xi}\right)^{-\beta}\frac{dp_c}{d\xi}\right] = 4\tau_{\text{path}}\left(\frac{ds}{d\xi}\right)^{\beta} p_c - \tau_{\text{path}}\frac{ds}{d\xi}p_c + \tau_s\frac{dp_c}{d\xi}$$

Transport/loss equation

diffusive transport | **Fermi-II** | **hadronic losses** | **streaming losses**

$$\frac{dp_c}{d\xi} + \xi_{\text{turb}}\frac{d^2s}{d\xi^2} = -\left(1 - f_{\text{gas}}\right)\frac{ds}{d\xi} - f_{\text{gas}}s\frac{ds}{d\xi}$$

Hydrostatic balance

CR pressure gradient | **turbulent pressure gradient** | **stellar gravity** | **gas self gravity**

+ 4 BCs

Coupled ODEs:

$$\tau_s \equiv \left(\frac{z_*}{\lambda_{c,*}}\right)$$

height of atmosphere

mfp to scattering

optical depth to scattering

$$\tau_{\text{path}} \equiv \frac{\tau_s \tau_{\text{pp}}}{\beta_{A,i}}$$

rectilinear optical depth

ion Alfven speed

optical depth to absorption over path

Coupled ODEs:

$$\tau_s \equiv \left(\frac{z_*}{\lambda_{c,*}}\right)$$

height of atmosphere

mfp to scattering

optical depth to scattering

$$\tau_{\rm path} \equiv \frac{\tau_s \tau_{\rm pp}}{\beta_{A,i}}$$

rectilinear optical depth

ion Alfven speed

optical depth to absorption over path

Coupled ODEs:

$$\tau_s \equiv \left(\frac{z_*}{\lambda_{c,*}}\right)$$

height of atmosphere

mfp to scattering

optical depth to scattering

$$\tau_{\text{path}} \equiv \frac{\tau_s \tau_{\text{pp}}}{\beta_{A,i}}$$

rectilinear optical depth

ion Alfven speed

optical depth to absorption over path

Coupled ODEs:

$$\tau_s \equiv \left(\frac{z_*}{\lambda_{c,*}}\right)$$

height of atmosphere

mfp to scattering

optical depth to scattering

$$\tau_{\text{path}} \equiv \frac{\tau_s \tau_{\text{pp}}}{\beta_{A,i}}$$

rectilinear optical depth

ion Alfven speed

optical depth to absorption over path

Coupled ODEs:

$$\tau_s \equiv \left(\frac{z_*}{\lambda_{c,*}}\right)$$

height of atmosphere

mfp to scattering

optical depth to scattering

$$\tau_{\text{path}} \equiv \frac{\tau_s \tau_{\text{pp}}}{\beta_{A,i}}$$

rectilinear optical depth

ion Alfven speed

optical depth to absorption over path

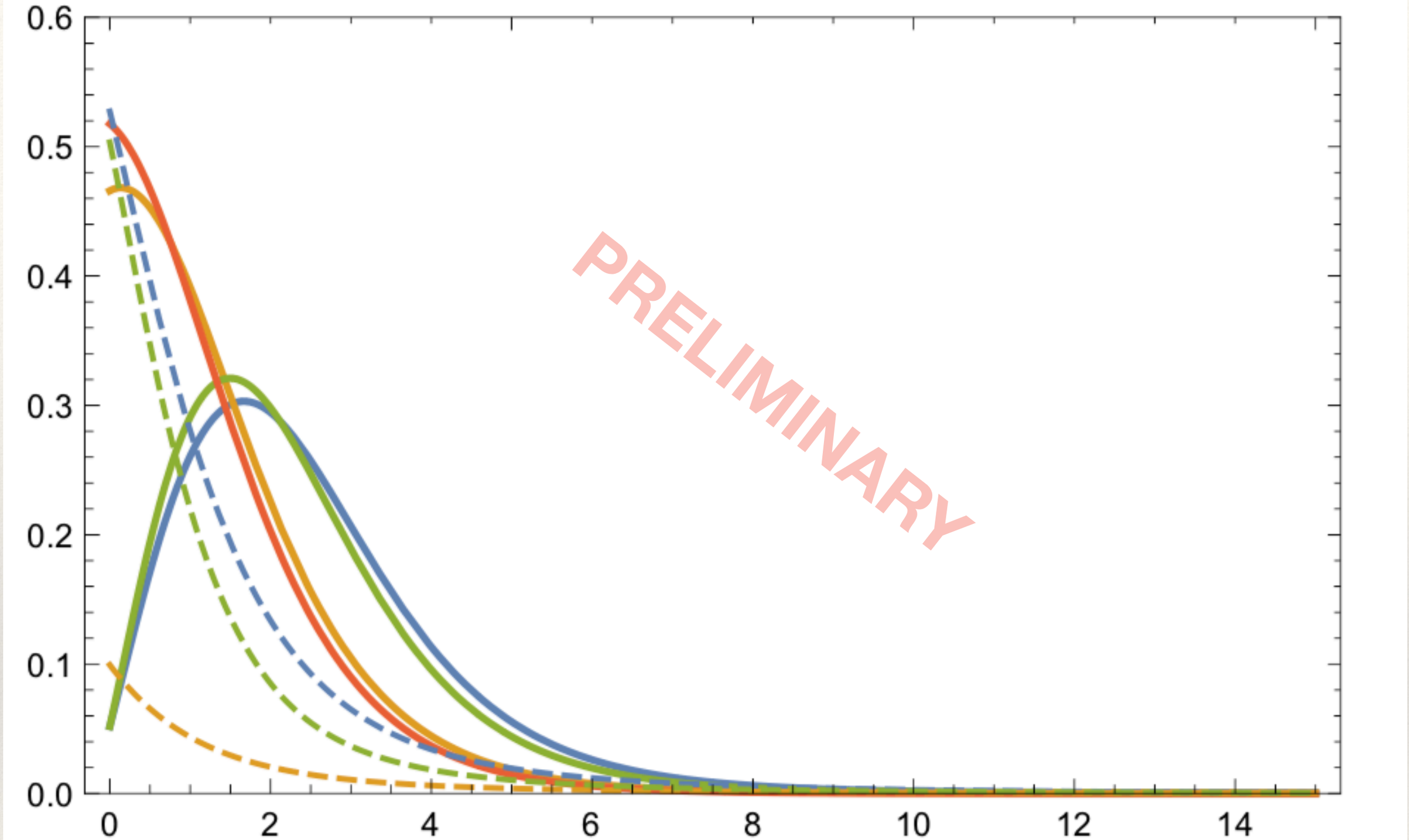

Numerical solutions give gas number density and cosmic ray pressure profiles

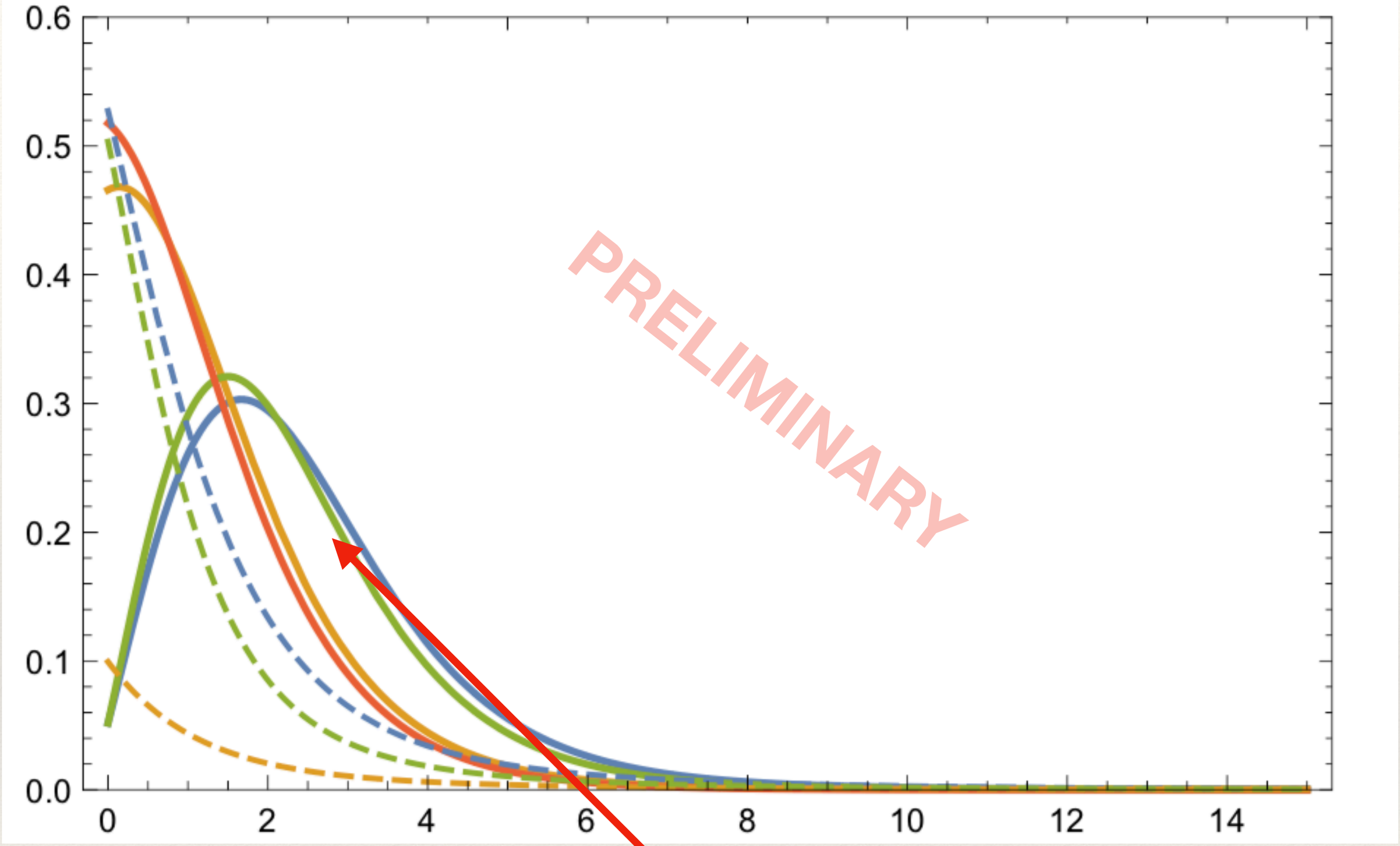

Numerical solutions give gas number density and cosmic ray pressure profiles

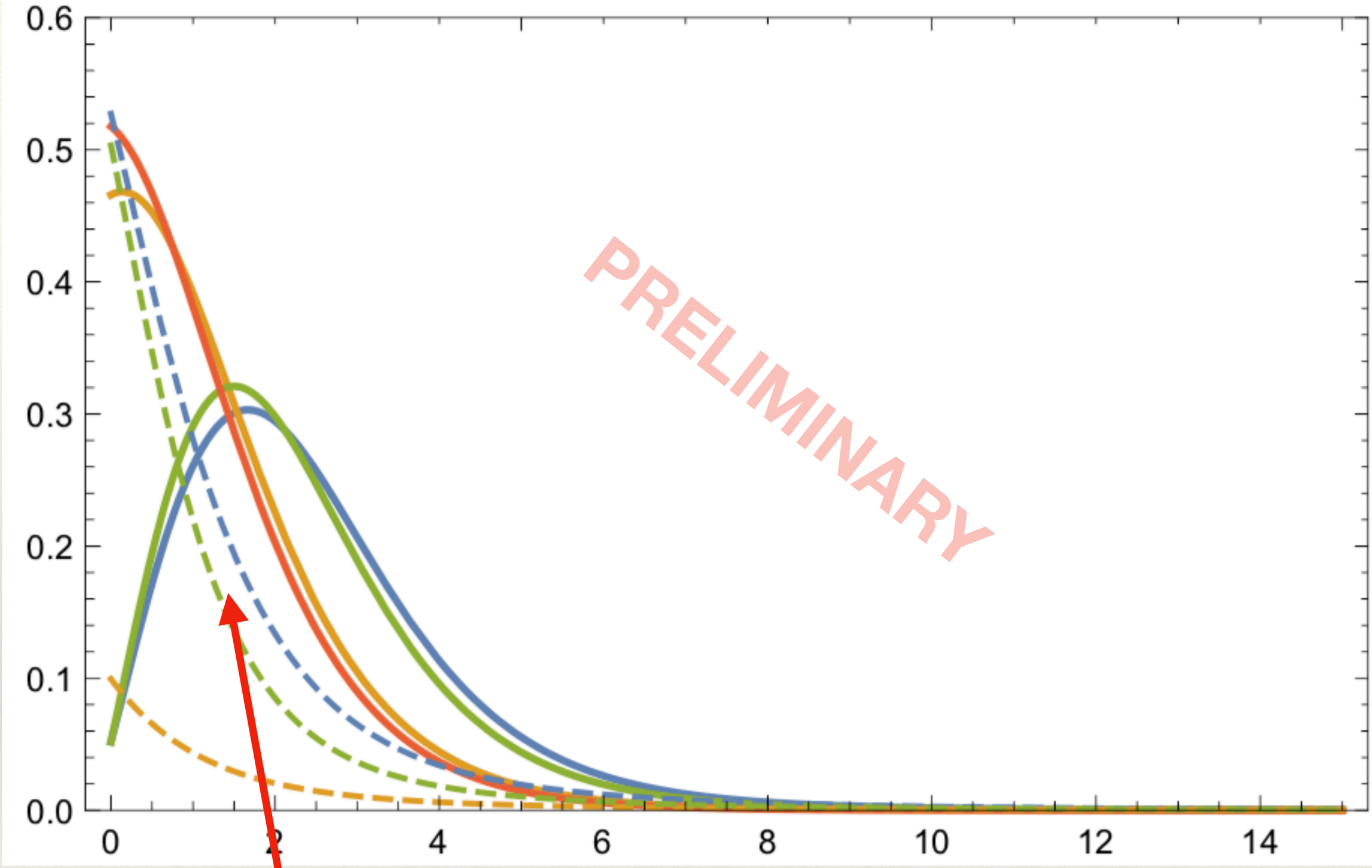

Numerical solutions give gas number density and cosmic ray pressure profiles

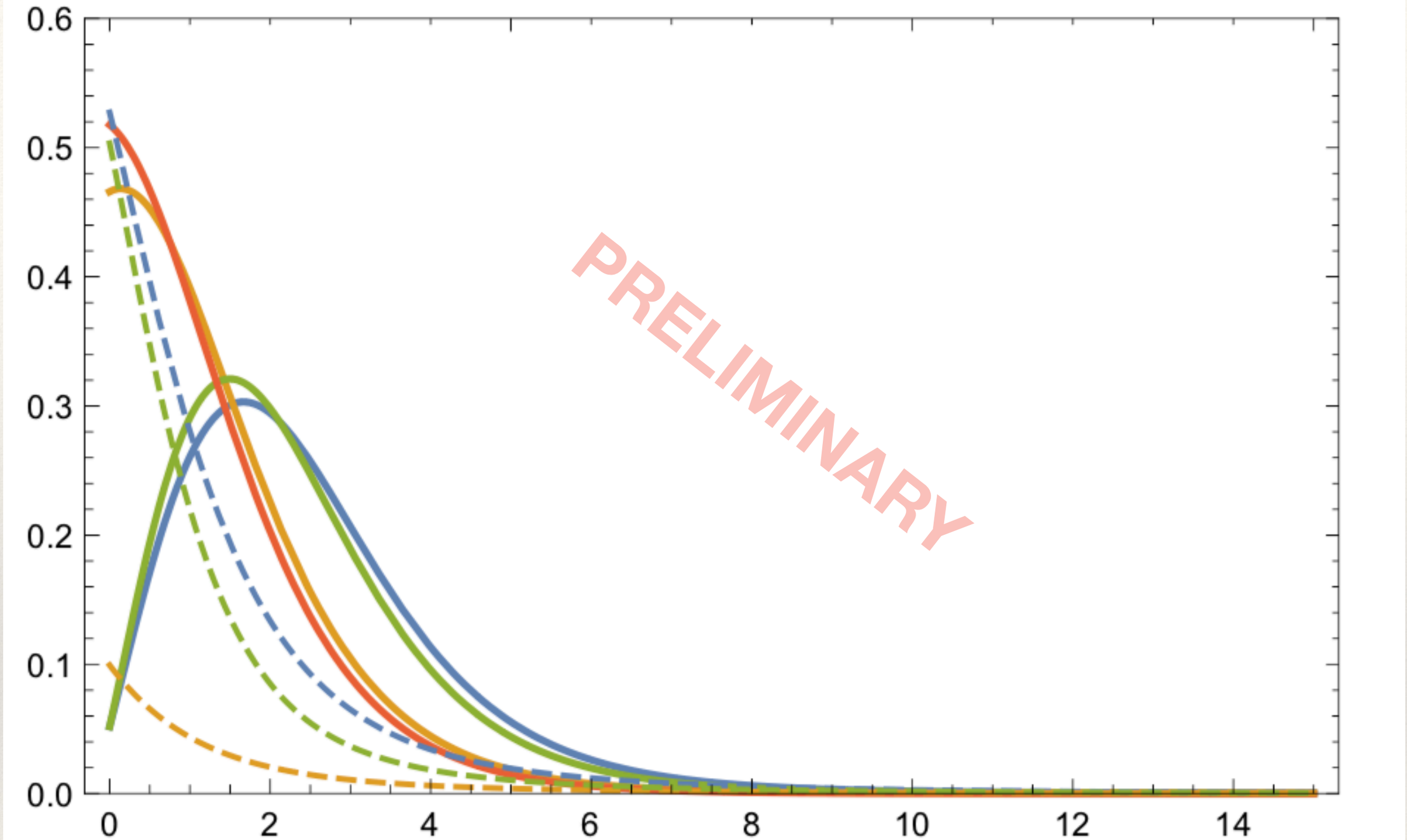

Numerical solutions give gas number density and cosmic ray pressure profiles

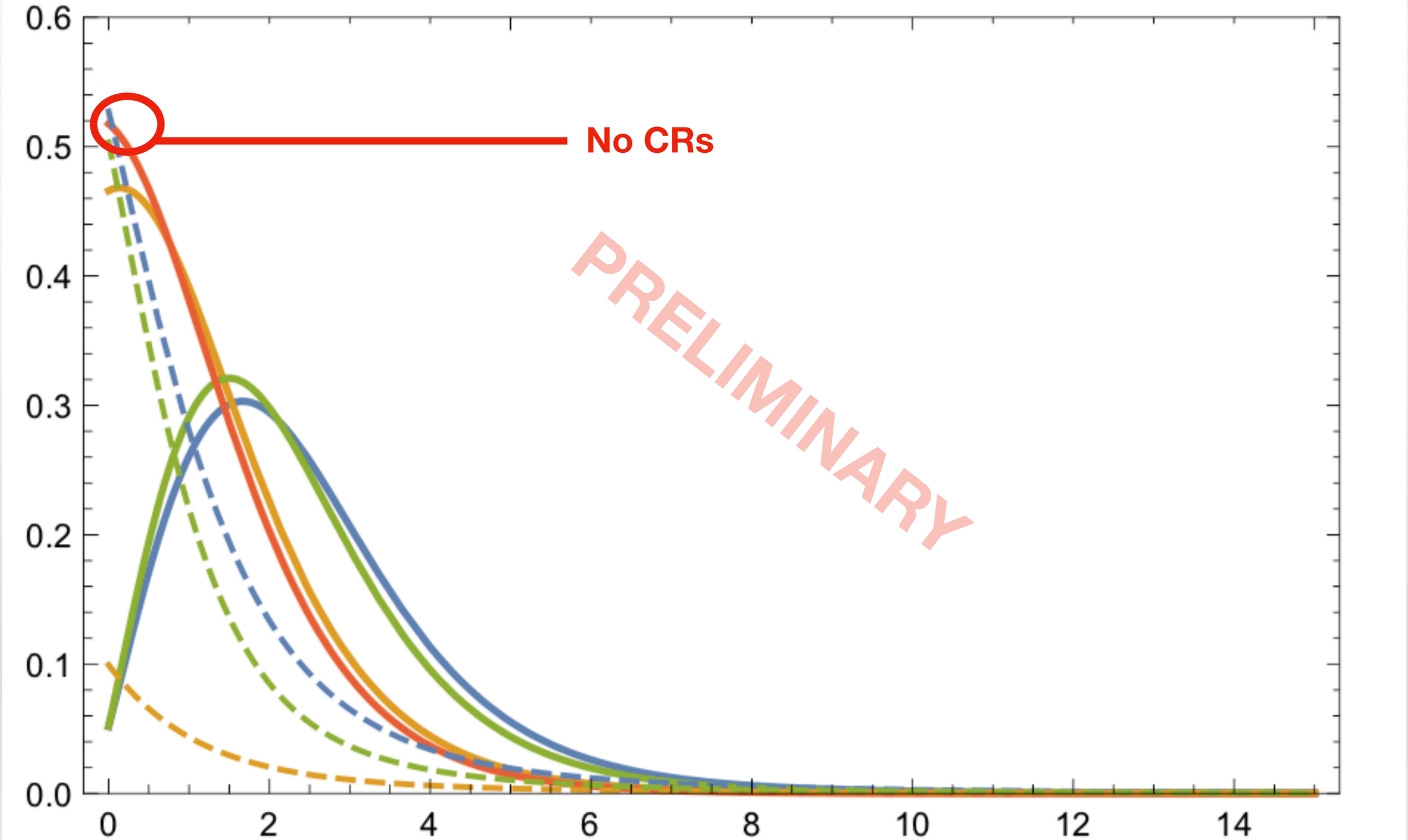

Numerical solutions give gas number density and cosmic ray pressure profiles

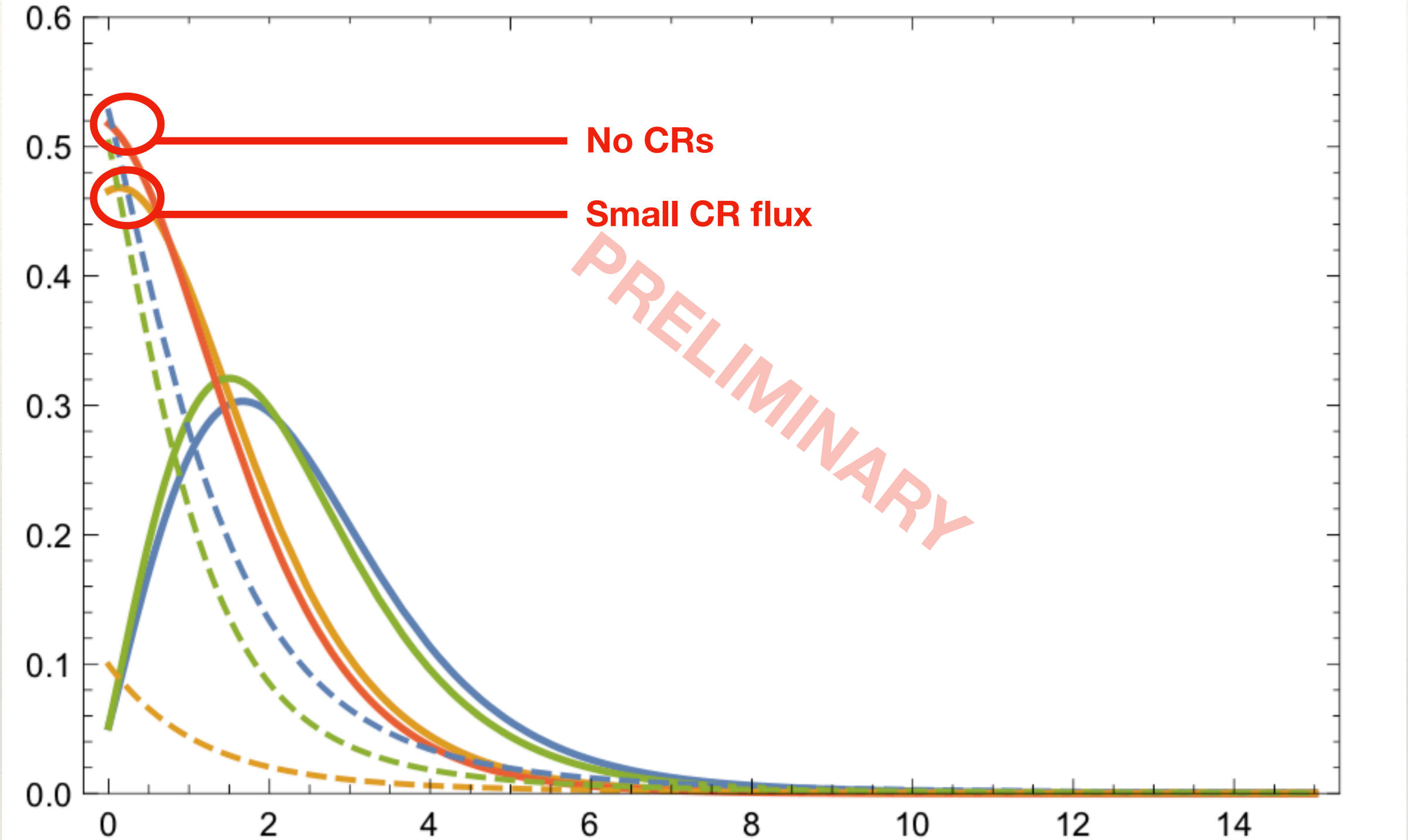

Numerical solutions give gas number density and cosmic ray pressure profiles

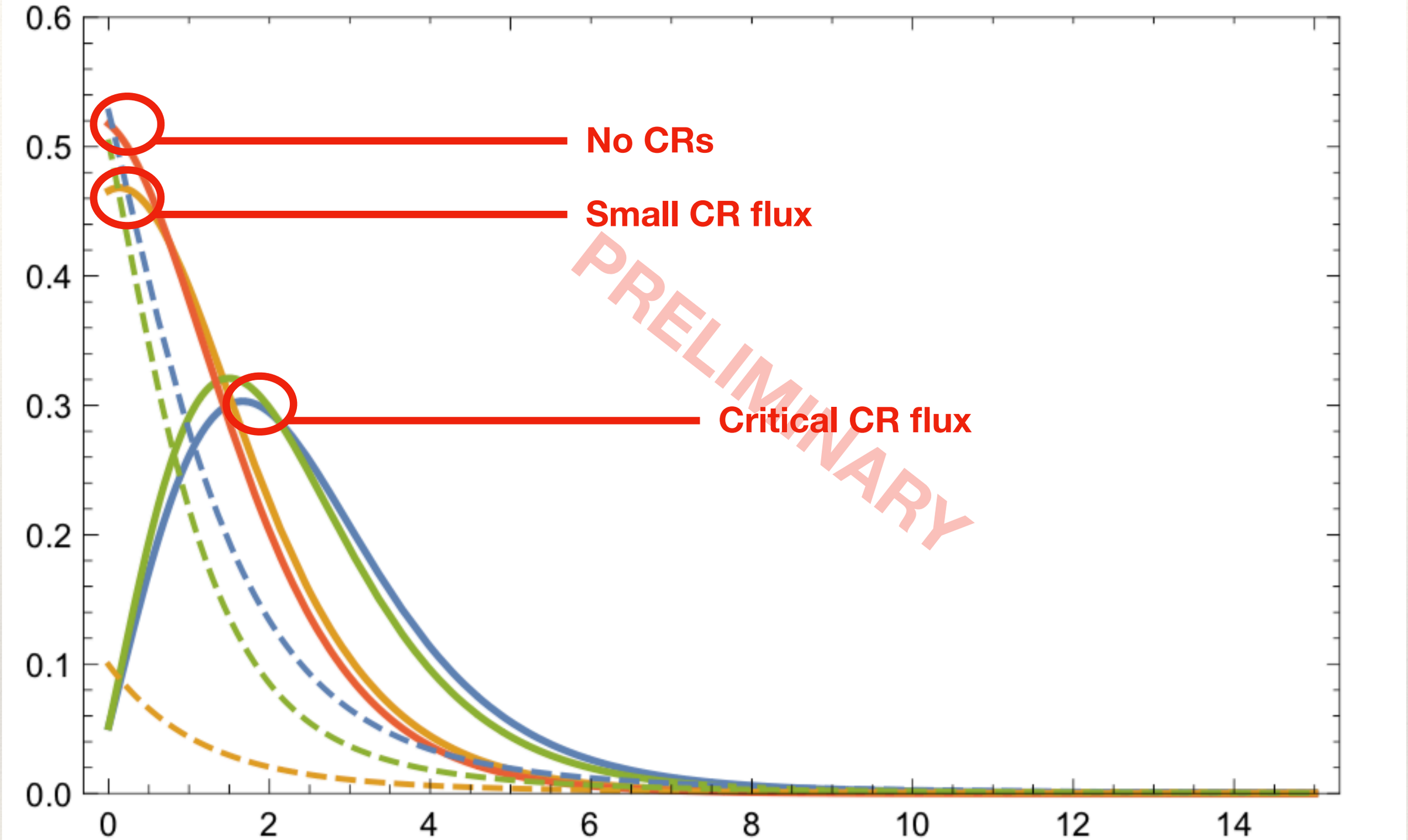

Numerical solutions give gas number density and cosmic ray pressure profiles

Star-forming Galaxies; Kennicutt-Schmidt Plane

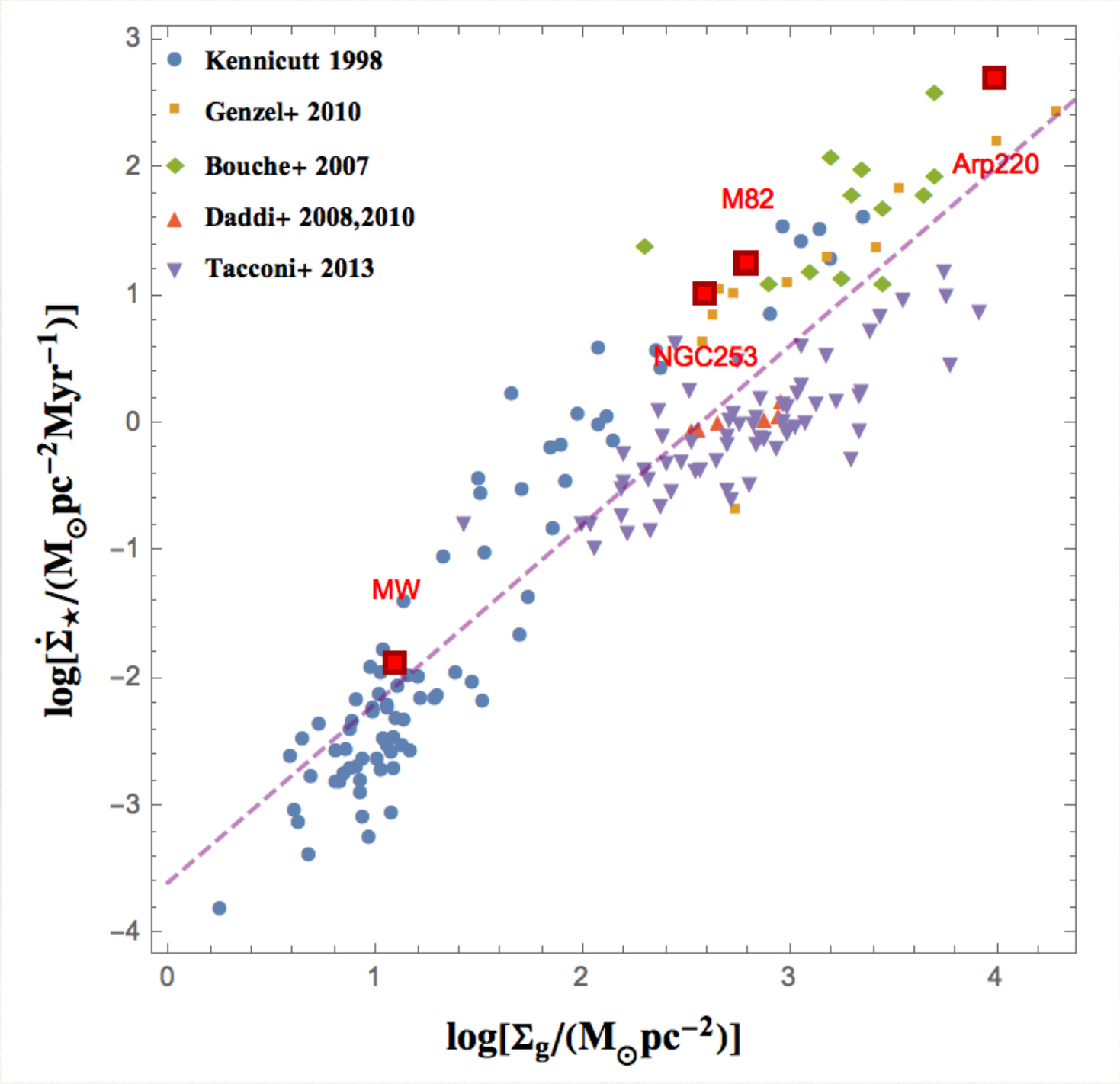

CR stability curve in physical parameter space:

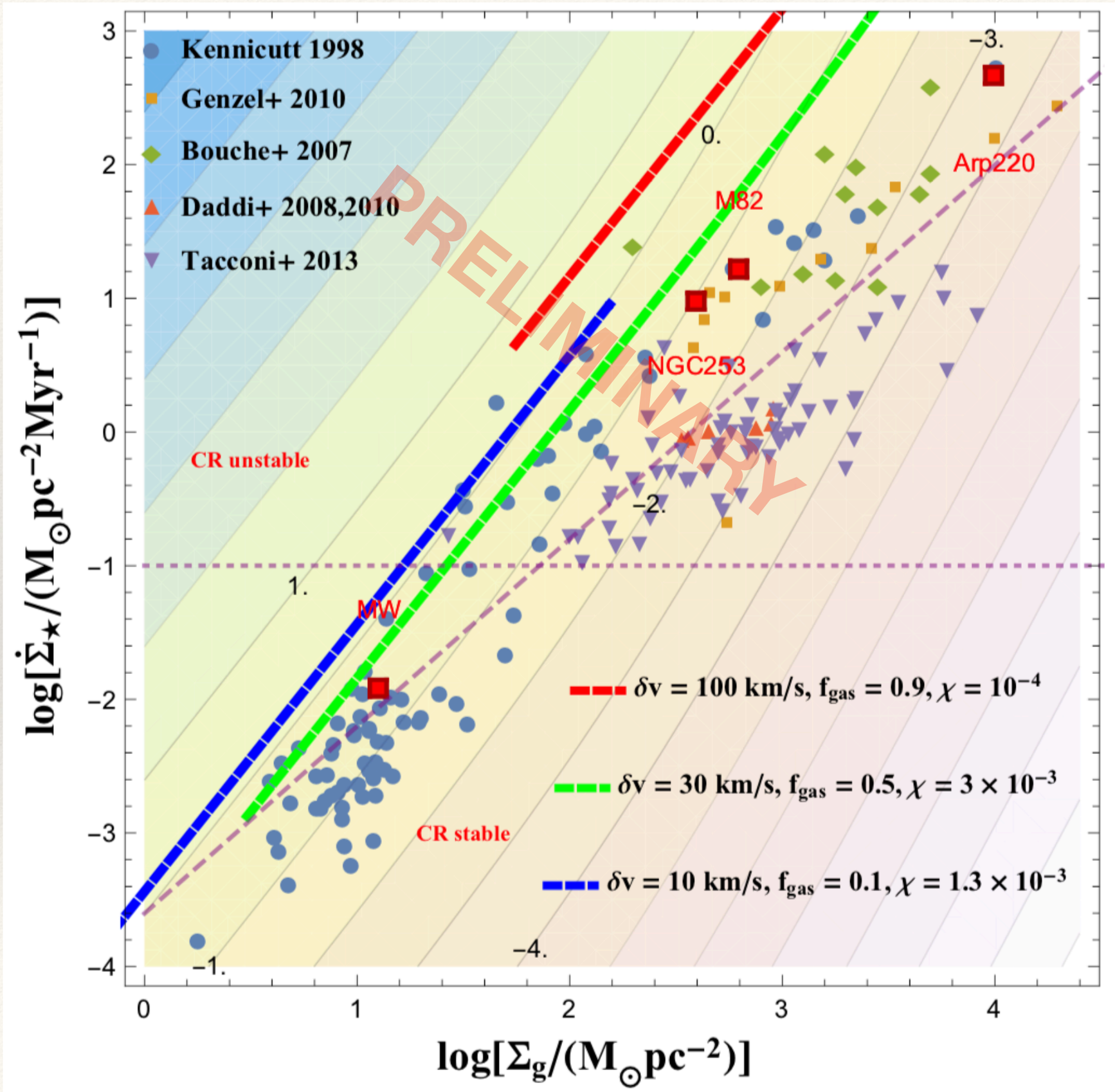

Hydrodynamic stability curves

CR stability curve in physical parameter space:

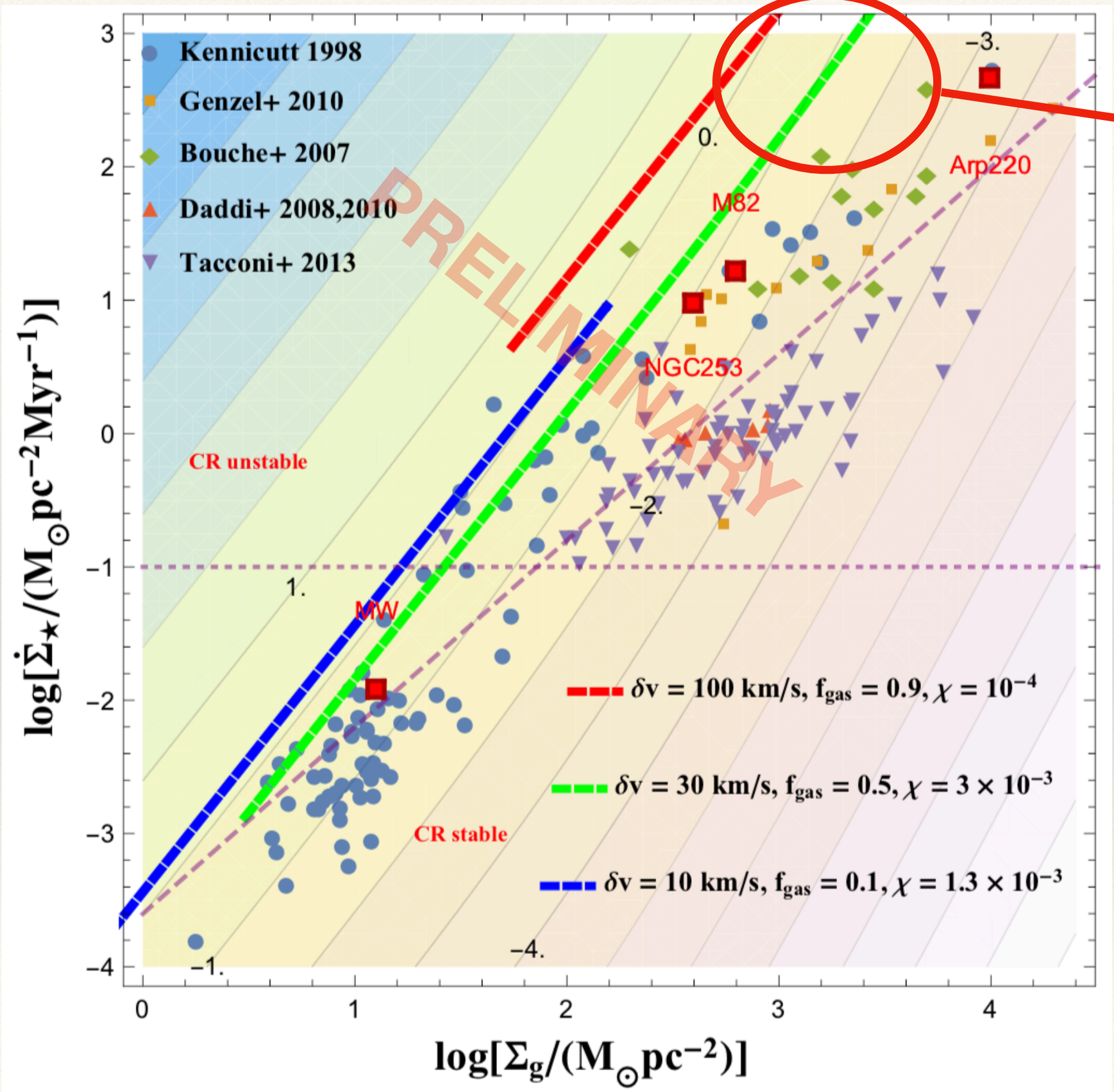

CRs NOT dynamically important in starbursts

Hydrodynamic stability curves

CR stability curve in physical parameter space:

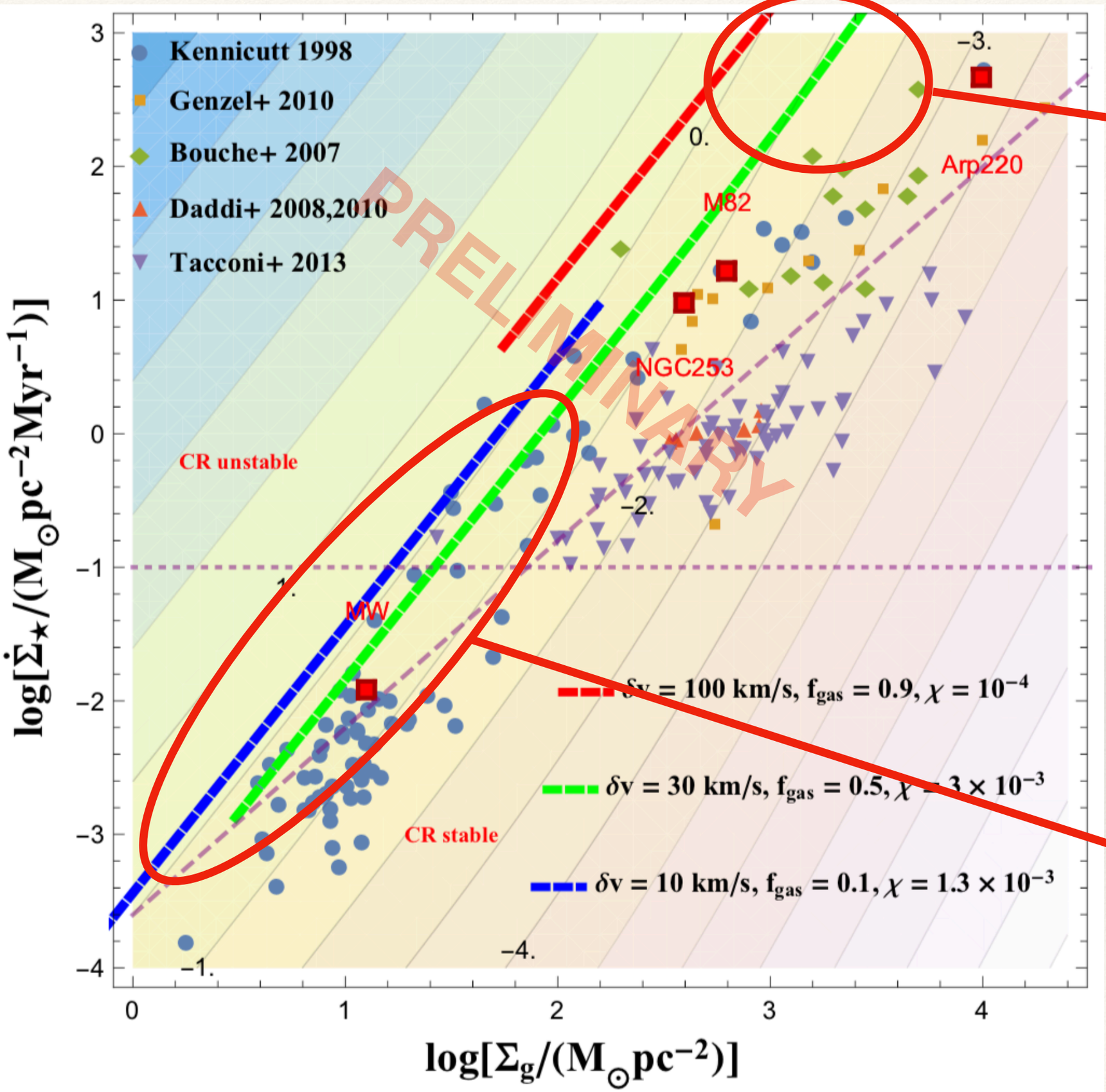

CRs NOT dynamically important in starbursts

Hydrodynamic stability curves

CRs dynamically important in 'ordinary' galaxies

Summary

Part I:

- In the dense, star-forming ISM phase, ~GeV CR transport is described by field line random walk at the **ion** Alfven speed v_{Ai}
- Implies energy-independent diffusion for GeV-TeV CRs in starbursts

Part II:

- The CR flux due to star formation can become so large that it precludes a hydrostatic equilibrium
- For 'normal' star-forming galaxies ($\Sigma_{gas} < 10^{2.5}\,M_\odot/pc^2$), CR feedback bounds the star formation rate surface density